Resource Allocation via Max-Min Goodput Optimization for BIC-OFDMA Systems

Riccardo Andreotti[1], Tao Wang[2], Vincenzo Lottici[1],
Filippo Giannetti[1], and Luc Vandendorpe[3]

***Abstract*— In this paper, a novel resource allocation (RA) strategy is designed for the downlink of orthogonal frequency division multiple access (OFDMA) networks employing practical modulation and coding under quality of service constraints and retransmission techniques. Compared with previous works, two basic concepts are combined together, namely, *i*) taking the goodput (GP) as performance metric, and *ii*) ensuring maximum fairness among users. The resulting RA maximizes thus the GP of the worst user, optimizing subcarrier allocation (SA), per-subcarrier power allocation (PA), and adaptation of modulation and coding (AMC) of the active users, yielding a nonlinear nonconvex mixed optimization problem (OP). The intrinsic demanding difficulty of the OP is tackled by iteratively and optimally solving the AMC, PA and SA subproblems, devoting special care to the demanding nonlinear combinatorial SA-OP. First, the optimal (yet computationally complex) solution is found by applying the branch&bound method to the optimal SA solution found in the relaxed domain, and accordingly, it is taken as benchmark. Then, an innovative suboptimal yet efficient solution based on the metaheuristic ant colony optimization (ACO) framework is derived. The proposed RA strategy is corroborated by comprehensive simulations, showing improved performance even at the cost of affordable numerical complexity.**

***Index Terms*— Orthogonal frequency division multiple access (OFDMA), bit-interleaved coded modulation, automatic repeat request (ARQ), goodput, resource allocation, max-min optimization problem, ant colony optimization.**

I. Introduction

Due to its high spectral efficiency, flexibility and capability of coping with harsh multipath fading, the orthogonal frequency division multiple access (OFDMA) is actually identified as a strong player for both current standardized 4G and beyond-4G high data rate wireless packet networks [1], [2], [3]. In order to fully exploit the potential of OFDMA in the downlink multiuser scenario, however, the base station (BS) must choose the best configuration of transmission parameters (TPs) by way of a properly designed resource allocation (RA) strategy, in accordance with the channel state information (CSI) and the quality of service (QoS) each user requires [4]. In this context, by virtue of the independent fading suffered by the users placed in different locations, the *multiuser diversity* takes a significant role in that, when a subcarrier of a given user deeply fades, it may be instead in good conditions for a different user [5]. Hence, for each packet to transmit, the BS can dynamically perform [1], [4]: *i)* subcarrier allocation (SA) to users, and for each user *ii)* power allocation (PA) across the subcarriers, combined with *iii)* adaptive modulation and coding (AMC). The total result is that the data rate conveyed by the subcarriers with better conditions can be increased through a suitable mix of power levels, modulation order and coding rate, thus optimizing the overall usage of the available resources.

Prior Works. The literature about RA for the downlink of OFDMA dates back to the works based on minimizing the overall transmit power consumption while maintaining the user data rate requirement [6], or alternatively, maximizing the data rate achieved by all the users subject to the total BS transmit power constraint [7]. The problem of possible unfair resource assignment to users with poor CSI is avoided resorting to proportional fairness [8] or maximum fairness [9], [10]. The previous works are then extended to a two-hop relaying scheme [11] and the downlink of coordinated multi-cell OFDMA scenarios [12]. Worth of being pointed out, [8]-[12] follow an information-theoretic approach, i.e., they adopt the user sum-rate as performance metric, thereby assuming unpractical infinite-length Gaussian codebooks.

Conversely, whenever discrete modulation formats and practical coding schemes, such as bit interleaved coded modulation (BICM) [13], are employed (on top of them) along with automatic repeat request (ARQ) retransmission mechanism to delivery error-free packets [14] (as typically required in data, broadcast and video streaming applications), the story is quite different. The conventional sum-rate metric is no longer meaningful in that the penalty of packet errors is not accounted for, and so, a different approach is called for. A more appropriate utility function capable of trading off the data rate achieved at physical (PHY) layer against the error rate suffered at data link (DL) layer, indeed, is embodied by the goodput (GP) metric, which is defined as the number of error-free payload bits delivered to the user by unit of time, or equivalently, the offered layer 3 data rate [15]. This explains the reason why the design of cross-layer RA strategies via the optimization of a GP-based utility function is gaining more and more interest, as shown in the sequel.

A considerable effort is first made in [16]-[17], although

[1]Department of Information Engineering, University of Pisa, I-56122 Pisa, Italy.
[2]Key Laboratory of Specialty Fiber Optics and Optical Access Network, Shanghai University, 200072, Shanghai, P. R. China.
[3]Communications and Remote Sensing Laboratory, Université Catholique de Louvain, B-1348 Louvain-la-Neuve, Belgium.
R. Andreotti, V. Lottici and F. Giannetti acknowledge the partial support of the PRA 2016 research project 5GIOTTO funded by the University of Pisa.
T. Wang′s work is supported by NSFC-61401266 and Innovation Program 14ZZ096.
L. Vandendorpe would like to thank BELSPO for funding the IAP BESTCOM network.

such works incur into a few restrictions or drawbacks: *i*) a high-SNR approximation of the subcarrier packet error rate (PER) is employed whereas the packets of each user are conveyed by a single subcarrier, thus underusing the potentials of *multiuser diversity* [16], [18]; *ii*) the BS transmits a single packet across all the subcarriers within each slot packet interval [19]; *iii*) while the users' outage probability is constrained to a target level, the objective to be optimized depends on the scheduled rates over the subcarriers and users [20], [21]; *iv*) in the amplify-and-forward relay-assisted OFDMA network proposed in [17], the potential of multiuser diversity is fully exploited only on condition that the number of the relays grows (impractically) faster than the number of users. *v*) the penalty induced by the packet errors is captured by using the outage probability (a quantity depending on the instantaneous mutual information) included within the definition of the GP expression adopted in [19]-[17]; *vi*) in all works, the available resources are assigned while starving those users with poor quality channel conditions and boosting the good ones.

At the other side, the cross-layer RA scheme proposed in [22] optimizes the sum of the users' GP achieved per transmitted frame, incorporating fairness among users. Herein, assuming perfect CSI at the BS, the GP expression is heuristically modeled as a function of the per-subchannel PER, which in turn is approximated, for a given user, as the average of the uncoded bit error rate (BER) across the assigned subcarriers. The search for the optimal subchannel, modulation and power allocation maximizing the GP metric turns out to be computationally involved, the corresponding OP being a nonlinear mixed integer programming (IP) problem. Nevertheless, applying the decomposition theory reduces the complexity without introducing an appreciable performance loss. In order to simplify the corresponding OP, however, in [22]: *i*) hard-decision Viterbi decoding is assumed; *ii*) the available subcarriers are evenly grouped in a number of subchannels, and consequently, subchannel, instead of subcarrier, allocation is performed; *iii*) proportional fairness cares about the performance of the worst user without any optimization; *iv*) the GP is modeleld by an "ad-hoc" expression depending on a given approximation of the BER function; *v*) the coding rate adopted within the transmitted packet is not optimized but a-priori chosen; *vi*) to decouple the original OP, the total power constraint is relaxed, by equally distributing the power among the subchannels instead of optimizing the power distribution among the subcarriers.

Rationale and Contributions. This paper deals with a cross-layer RA scheme for the downlink of a BIC-OFDMA network employing ARQ retransmission, under the QoS constraint on the users' PER and assuming ideal CSI at the BS. The idea behind the proposed scheme is to maximize the minimum among users' GP, so guaranteeing maximum fairness among users, via the optimal choice of the AMC, SA and PA strategies. So doing, the restrictions on the subcarrier and power allocation made in [22] are avoided. In view of the following key features, our proposal comes out to be more competitive when compared to the existing literature.

1) Two pivotal concepts are properly combined together: *i*) taking the *expected GP*, or EGP[1], performance metric as objective function, and *ii*) ensuring *maximum fairness* among users. Hence, dissimilarly from [22], our approach, referred to in the sequel as "max-min GP", or MMG for short, consists in searching for the optimal TPs configuration, i.e., SA to users, PA and modulation to subcarriers, and coding rate, in such a way that the EGP of the worst performing user is maximized at each ARQ round.
2) With the aim of building a computationally reasonable RA scheme, the *actual GP*, or AGP[2] is estimated exploiting a manageable expression of the EGP metric. The result is obtained by resorting to the κESM performance prediction model recently derived in [23] and successfully applied in [24] for single-user BIC-OFDM links. The rationale of such an approach consists in an in-depth characterization of the log-likelihood ratio (LLR) metrics required by the *soft* Viterbi decoder, thanks to which the received SNRs over the subcarriers are simply and accurately mapped into a closed-form scalar, the so-called effective SNR (ESNR); see Sect. III-A for more details.
3) The MMG results a nonlinear nonconvex OP with mixed integer- and real-valued variables, and accordingly, searching for its global optimum solution is inherently prohibitive. Nevertheless, the rationale of the *viable* approach we pursue is to subdivide the original OP into three subproblems, i.e, the AMC-OP, PA-OP and SA-OP. Then, the conventional iterative coordinate ascent method (CAM) is applied [25], wherein at a given iteration each subproblem is optimally and consecutively solved at affordable complexity.
4) While the AMC-OP is easily solved via exhaustive search and the PA-OP is handled by the conventional Lagrangian dual decomposition (LDD) theory [26], the SA-OP is a demanding NP-hard nonlinear IP problem. Two solving algorithms, however, help us skipping the above issue. One is optimal yet with high complexity: first, the SA-OP is relaxed in a continous domain, solved, and then, optimally brought to the discrete domain by means of the branch and bound (B&B) algorithm [27]. As a consequence, it will be used for performance benchmark only. The second one, instead, works as an efficient accuracy-versus-complexity tradeoff: it is motivated by the *metaheuristic ant colony optimization* (ACO) framework [28], which has been contemplated in [29] in a very preliminary form for a cognitive OFDMA system.
5) For the sake of simplicity, the MMG-OP is formulated assuming ideal CSI at the BS and the absence of any form of maximum ratio combing (MRC) at the receiver. It can be proved, however, that the MMG-RA can easily take care of the above issues by properly modifying the expression of the κESM prediction model only. So

[1]The EGP is defined as the statistical expectation of the GP, evaluated over the TPs at the BS transmitter.

[2]The AGP is defined as the actual GP metric measured through numerical simulations over realistic wireless environments.

doing, we get a RA strategy that is based on the same solving structure, even exhibiting the advantage of better performance and robustness while ensuring maximum fairness among the active users.

6) Comprehensive simulations over realistic propagation scenarios support our analytical findings. Due the lack in the literature of similar RAs addressing the topics of our interest, we adopt as for performance benchmark the heuristic RA algorithm formulated in Sect. VI-D, which is employed to initialize the CAM procedure as well. Although the MMG-based RA originally requires an unfeasible computational load, a suitable mix of modeling and OP design enables a viable scheme supplying notable performance improvements over non adaptive strategies.

Organization. Section II describes the BIC-OFDMA system model and Sect. III formulates the MMG-OP. In Sections IV and V, the methods to solve the PA- and AMC-OPs and the SA-OP are outlined, respectively, while the simulation results are discussed in Sect. VI. Finally, some concluding remarks are drawn in Sect. VII.

Notations. Matrices are in upper case bold while column vectors are in lower case bold, $[\cdot]^T$ is the transpose of a matrix or a vector, $\times$ is the Cartesian product, calligraphic mathematical symbols, e.g., $\mathcal{A}$, represent sets, $|\mathcal{A}|$ is the cardinality of $\mathcal{A}$, $\mathcal{A}(i)$ is the ith element of $\mathcal{A}$, $\mathcal{A}^N \triangleq \underbrace{\mathcal{A} \times \mathcal{A} \times \cdots \times \mathcal{A}}_{N}$ is the Cartesian power of order N, $\|\mathbf{a}\| \triangleq \sqrt{\mathbf{a}^T\mathbf{a}}$ is the ℓ_2-norm of $\mathbf{a}$, $f \circ g$ represents the composition of functions f and g, the gradient of the function $F(\mathbf{x})$ evaluated in $\overline{\mathbf{x}}$, with $\mathbf{x}, \overline{\mathbf{x}} \in \mathbb{R}^N$, is identified as $\nabla_{\mathbf{x}} F(\overline{\mathbf{x}})$, $\lceil x \rceil$ is the nearest greater integer to x, $x^{(i)}$ is the value of the variable x at the iteration i, $[x]_a^b$ means x if $a < x < b$, $x = a$ ($x = b$) if $x < a$ ($x > b$), $[\mathbf{x}]_{\mathcal{D}_\mathbf{x}}$ is the component-wise projection of the elements of $\mathbf{x}$ over the set $\mathcal{D}_\mathbf{x}$, and $\mathrm{E}_x\{\cdot\}$ is the statistical expectation with respect to (w.r.t.) the random variable (RV) x.

II. System Model

We consider the downlink from a BS to Q user receivers (also called network load) with indexes in $\mathcal{Q} \triangleq \{1, \cdots, Q\}$, employing the BIC-OFDMA signaling format. The Q BS-to-user links share the band B which is divided into N subcarriers indexed by the elements of $\mathcal{N} \triangleq \{1, \cdots, N\}$. Each packet of user $q \in \mathcal{Q}$ coming from the upper layers of the stack (typically, an Internet Protocol packet or layer-3 control signaling message), with length $N_q^{(\mathrm{u})} = N_q^{(\mathrm{h})} + N_q^{(\mathrm{p})} + N_q^{(\mathrm{CRC})}$, i.e., comprising the header, payload and cyclic redundancy check (CRC) bits, respectively, is encoded using a linear coding scheme with mother code $\bar{r}_0$. At the ℓth ARQ protocol round[3] (PR), with $\ell \in \mathcal{L} \triangleq \{1, \cdots, L\}$, the encoded bits are first punctured according to the coding rate $r_{\ell,q} \in \mathcal{D}_\mathrm{r} \triangleq \{\tilde{r}_0, \cdots, \tilde{r}_{\max}\}$ assigned to the user q, thereby obtaining $N_{\ell,q}^{(\mathrm{c})} \triangleq N_q^{(\mathrm{u})}/r_{\ell,q}$ punctured encoded bits. Then, they are randomly processed by the bit-level interleaver in accordance with the BICM scheme.

Let us designate at PR $\ell \in \mathcal{L}$: *i*) the SA vector with $\mathbf{a}_{\ell,q} \triangleq [a_{\ell,q,1}, \cdots, a_{\ell,q,N}]^T \in \mathcal{D}_\mathrm{a}^N$, where $\mathcal{D}_\mathrm{a} \triangleq \{a_{\ell,q,n} \,|\, a_{\ell,q,n} \in \{0,1\}, \forall n \in \mathcal{N}, \forall q \in \mathcal{Q}, \forall \ell \in \mathcal{L}\}$, $a_{\ell,q,n}$ being the indicator function for the subcarrier n, i.e., $a_{\ell,q,n} = 1$ if subcarrier n is assigned to user q, and zero otherwise, so that $\sum_{q\in\mathcal{Q}} a_{\ell,q,n} \leq 1$, $\forall n \in \mathcal{N}$, thus meaning that each subcarrier is assigned at most to one user at a time; *ii*) the number of bits loaded[4] by user q on each of its subcarriers with $m_{\ell,q} \in \mathcal{D}_\mathrm{m} \triangleq \{2, \cdots, m_{\max}\}$.

The punctured and interleaved bits obtained above are grouped into $m_{\ell,q}$-tuples, which are one-to-one mapped to the sequence $\{s_{\ell,q,i}\}$, $1 \leq i \leq \left\lceil N_{\ell,q}^{(\mathrm{c})}/m_{\ell,q} \right\rceil$, of unit-energy symbols belonging to a $2^{m_{\ell,q}}$-QAM constellation. Thus, at the generic OFDM symbol, the $N_{\ell,q}^{(\mathrm{s})} \triangleq \sum_{n\in\mathcal{N}} a_{\ell,q,n}$ positions of $\mathbf{x}_\ell \triangleq [x_{\ell,1}, \cdots, x_{\ell,N}]^T$ having indexes $n \in \mathcal{N}_{\ell,q} \triangleq \{n \in \mathcal{N} \,|\, a_{\ell,q,n} = 1, \forall q \in \mathcal{Q}, \forall \ell \in \mathcal{L}\}$, such that $\bigcup_{q\in\mathcal{Q}} \mathcal{N}_{\ell,q} \subseteq \mathcal{N}$, $\forall \ell \in \mathcal{L}$, are loaded with one block of consecutive modulation symbols read from $\{s_{\ell,q,i}\}$, properly scaled by $\sqrt{p_{\ell,n}}$ (chosen according to the adopted PA strategy), where $p_{\ell,n} \in \mathcal{D}_\mathrm{p} \triangleq \{p_{\ell,n} \in \mathbb{R} \,|\, 0 \leq p_{\ell,n} \leq P, \forall n \in \mathcal{N}, \forall \ell \in \mathcal{L}\}$ is the fraction of the total power P available at the BS, such that $\sum_{n\in\mathcal{N}} p_{\ell,n} \leq P$. Eventually, the scaled modulation symbols corresponding to the Q active users are transmitted using the OFDM format over a frequency-selective block-fading channel.

At the receiver, after cyclic prefix removal and FFT processing, the signal sample received at round ℓ on subcarrier n assigned to user q results as

$$z_{\ell,q,n} = a_{\ell,q,n}\sqrt{p_{\ell,n}} h_{\ell,q,n} x_{\ell,n} + w_{\ell,q,n}, \quad \forall n \in \mathcal{N}_{\ell,q}, \forall q \in \mathcal{Q}, \forall \ell \in \mathcal{L}, \quad (1)$$

where $h_{\ell,q,n}$ is the complex-valued multipath channel coefficient related to the link connecting the BS to the qth user, whereas $w_{\ell,q,n}$ is the noise component, which is modeled as a zero-mean complex-valued Gaussian-distributed RV with variance $\sigma^2_{\ell,q,n}$. From (1), the signal-to-noise-ratios (SNRs) over the channels relevant to the subcarriers assigned to user q are collected by $\boldsymbol{\gamma}_{\ell,q} \triangleq [\gamma_{\ell,q,1}, \cdots, \gamma_{\ell,q,N}]^T$, where $\gamma_{\ell,q,n} \triangleq p_{\ell,n} \dfrac{|h_{\ell,q,n}|^2}{\sigma^2_{\ell,q,n}}$, $\forall n \in \mathcal{N}_{\ell,q}$, and without loss of generality (w.l.g.) $\gamma_{\ell,q,n} \triangleq 0$, $\forall n \notin \mathcal{N}_{\ell,q}$, $\forall q \in \mathcal{Q}$ and $\forall \ell \in \mathcal{L}$.

III. Resource Allocation based on Max-Min Goodput Optimization

In this section, we first derive the EGP metric for the ARQ-based BIC-OFDMA system outlined in Sect. II. Then, we formulate the MMG-OP, which optimizes the EGP objective function under a number of given constraints.

[3] At a given transmission time, the ARQ mechanisms of the Q users may be at different number of PRs, meaning thus that the PR index ℓ depends on the user index q. To ease notation, however, in the following we will drop such a dependence.

[4] In the current work, for simplicity, the same modulation format is assumed for all the subcarriers assigned to each user, that is to say, $m_{\ell,q}$ is independent of the subcarrier index n; see further comments in Sect. IV-B. Nevertheless, in the proposed RA strategy, the frequency diversity effect is exploited concerning the SA to users and PA across the subcarriers.

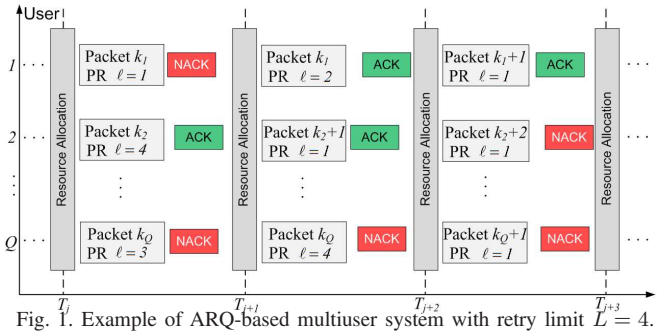

Fig. 1. Example of ARQ-based multiuser system with retry limit $L = 4$.

A. The Expected Goodput Objective Function

The lack of a reliable knowledge about the channel coefficients $\mathbf{h}_{\ell,q} \triangleq [h_{\ell,q,1} \cdots, h_{\ell,q,N}]^T$ for all users and in the future PRs prevents the BS from the *joint* optimization, at the beginning of each packet transmission, of the TPs $\boldsymbol{\tau}_{\ell,q} \triangleq \{\mathbf{p}_\ell, \mathbf{a}_{\ell,q}, m_{\ell,q}, r_{\ell,q}\}$, $\forall \ell \in \mathcal{L}$ and $\forall q \in \mathcal{Q}$, where $\mathbf{p}_\ell \triangleq [p_{\ell,1}, \cdots, p_{\ell,N}]^T \in \mathcal{D}_{\rm p}^N$; as for the definition about the TPs, see Sect. II. Hence, inspired by the works [18] and [24] (though proposed in different contexts), an alternative yet effective route is pursued, which consists of a *per-round optimization*, as sketched in Fig. 1. The idea is quite simple: at PR ℓ we adapt the TPs $\boldsymbol{\tau}_{\ell,q}$ to the *current* channel conditions regardless of the *future* channel evolution, till the packet is successfully decoded or the PR retry limit L is reached. Based upon a lower bound (LB) of the EGP metric, as derived in Appendix A, the objective function is expressed by the following formula

$$\zeta_{\ell,q}(\boldsymbol{\tau}_{\ell,q} \,|\, \mathbf{h}_{\ell,q}) \triangleq \frac{N_q^{(\rm p)}}{N_q^{(\rm u)}} r_{\ell,q}\, m_{\ell,q} \sum_{n\in\mathcal{N}} a_{\ell,q,n} \left[1 - \Gamma_{r_{\ell,q}}(\boldsymbol{\tau}_{\ell,q}|\mathbf{h}_{\ell,q})\right], \quad (2)$$

where $\Gamma_{r_{\ell,q}}(\boldsymbol{\tau}_{\ell,q} \,|\, \mathbf{h}_{\ell,q})$ is the packet error probability (PER) of user q at PR ℓ when the TPs vector $\boldsymbol{\tau}_{\ell,q}$ is used over the (known) channel response $\mathbf{h}_{\ell,q}$. Eq. (2), indeed, results as the number of information bits correctly received per packet by each user at each PR, referred to in the sequel as EGP.

The problem to solve now is the way the PER is evaluated when practical modulation and coding schemes are employed in presence of frequency-selective channels. Toward this end, we resort to the effective SNR mapping (ESN) technique [30]. This method considers an equivalent binary coded system working over additive white Gaussian noise (AWGN) channel and experiencing the effective SNR (ESNR) $\bar{\gamma}_{\ell,q}$, which maps the received SNRs $\boldsymbol{\gamma}_{\ell,q}$ (see the ending of Sect. II) and the TPs $\boldsymbol{\tau}_{\ell,q}$ in such a way that $\Gamma_{r_{\ell,q}}(\boldsymbol{\tau}_{\ell,q} \,|\, \mathbf{h}_{\ell,q}) = \Phi_{r_{\ell,q}}[\bar{\gamma}_{\ell,q}(\boldsymbol{\tau}_{\ell,q} \,|\, \mathbf{h}_{\ell,q})]$, where $\Phi_{r_{\ell,q}}(\cdot)$ is a monotonically decreasing and convex function in the range of interest, obtainable either in closed-form or by simulation.

Due to its accuracy and the simple mapping function, we specifically choose the κESM model formulated in [23]. Thus, upon fixing the PR index ℓ, dropping for simplicity the dependence of the various quantities on it, and observing that the OFDMA system is nothing but a set of Q independent and frequency-orthogonal OFDM users, the κESM ESNR corresponding to user q can be written as

$$\bar{\gamma}_q(\boldsymbol{\tau}_q \,|\, \mathbf{h}_q) \triangleq -\log\left\{\frac{\sum_{n\in\mathcal{N}} a_{q,n}\Omega_{q,n}(\mathbf{p}, m_q \,|\, \mathbf{h}_q)}{m_q \sum_{i\in\mathcal{N}} a_{q,i}}\right\}, \quad \forall q \in \mathcal{Q}, \quad (3)$$

with $\Omega_{q,n}(\mathbf{p}, m_q \,|\, \mathbf{h}_q) \triangleq \sum_{\mu=1}^{\sqrt{2^{m_q}}/2} \alpha_{q,\mu} \mathrm{e}^{-p_n \beta_{q,\mu} \frac{|h_{q,n}|^2}{\sigma_{q,n}^2}}$, where $\alpha_{q,\mu} \triangleq \eta_q(\mu)/2^{m_q-1}$, $\beta_{q,\mu} \triangleq [\mu d_q^{(\min)}/2]^2$, and $\eta_q(\mu)$ denotes the number of QAM symbols at distance $\mu d_q^{(\min)}$ from the nearest neighbor in the complementary subset[5], both $\eta_q(\mu)$ and $d_q^{(\min)}$ depending on the modulation order only; see [23] for further details. Thus, the BS evaluates $\bar{\gamma}_q$, $\forall q \in \mathcal{Q}$, and enters it in the look-up table which returns the values of the PER $\Phi_{r_{\ell,q}}$, for the selected coding rate, obtained by simulation.

B. Formulation of the Max-Min Goodput based Resource Allocation Problem

In view of Sect. III-A, the RA problem that maximizes the minimum among the user EGPs, we called in Sect. I as MMG for short, can be formulated as follows.

Definition 1 (MMG-OP): Assuming that the transmitter has perfect knowledge of the current CSI $\mathbf{h} \triangleq [\mathbf{h}_1^T, \mathbf{h}_2^T, \cdots, \mathbf{h}_Q^T]^T$ of all the users *at each PR*, the MMG-OP results as

$$\begin{aligned} \boldsymbol{\tau}^\star \;=\; & \arg\max_{\boldsymbol{\tau}\in\mathcal{D}_\tau} \xi(\boldsymbol{\tau} \,|\, \mathbf{h}) \\ \text{s.t.} \quad & \textstyle\sum_{n\in\mathcal{N}} p_n \le P, && \text{(a)} \\ & \textstyle\sum_{q\in\mathcal{Q}} a_{q,n} \le 1, \qquad \forall n \in \mathcal{N}, && \text{(b)} \\ & \Phi_{r_q}\left[\bar{\gamma}_q(\boldsymbol{\tau}_q \,|\, \mathbf{h}_q)\right] \le \Upsilon_q, \qquad \forall q \in \mathcal{Q}, && \text{(c)} \end{aligned} \quad (4)$$

with the objective function being expressed by

$$\xi(\boldsymbol{\tau} \,|\, \mathbf{h}) = \min_{q\in\mathcal{Q}} \{\zeta_q(\boldsymbol{\tau}_q \,|\, \mathbf{h}_q)\}, \quad (5)$$

where

$$\zeta_q(\boldsymbol{\tau}_q \,|\, \mathbf{h}_q) = \frac{N_q^{(\rm p)}}{N_q^{(\rm u)}} r_q\, m_q \sum_{n\in\mathcal{N}} a_{q,n} \left\{1 - \Phi_{r_q}\left[\bar{\gamma}_q(\boldsymbol{\tau}_q \,|\, \mathbf{h}_q)\right]\right\} \quad (6)$$

is obtained from EGP (2) after exploiting the κESM performance model, $\boldsymbol{\tau}^\star$ is the optimal solution with $\boldsymbol{\tau} \triangleq \{\boldsymbol{\tau}_1, \cdots, \boldsymbol{\tau}_Q\} \in \mathcal{D}_\tau \triangleq \mathcal{D}_{\rm p}^N \times \mathcal{D}_{\rm a}^{NQ} \times \mathcal{D}_{\rm m}^Q \times \mathcal{D}_{\rm r}^Q$, $\bar{\gamma}_q(\boldsymbol{\tau}_q \,|\, \mathbf{h}_q)$ is given by (3) and Υ_q is the QoS threshold below which the PER of user q has to be kept.

A few remarks are now in order.

1) The novelty of the formulation of the EGP (6) for our system, when compared to the literature, has to be properly emphasized. In a nutshell, the PER under a frequency-selective channel has been obtained resorting to the accurate κESM model proposed in [23], and not through a simple average of the BER per subcarrier. The key factor relies on the in-depth characterization of the LLR metrics at the input of the soft decoder, thus

[5]The complementary subset of a symbol $x \in \mathcal{X}$-QAM having the bit b at the kth label position is the subset of the constellation symbols having the bit b' at the kth label position, with b' being the complementary of b.

obtaining a simple and accurate mapping of the received SNRs over the subcarriers into a closed-form scalar.

2) The MMG-OP is a constrained nonlinear nonconvex OP with mixed integer- and real-valued variables. As a consequence, assembling an efficient numerical method to find the global optimum is *de facto* very demanding, whereas resorting to a naive exhaustive search is quite prohibitive [31, Ch. 6]. More in detail: *i*) the binary variables $a_{q,n}$, $\forall q \in \mathcal{Q}$ and $\forall n \in \mathcal{N}$, make the problem (4) have a combinatorial complexity exponentially increasing with NQ; *ii*) the objective function (5) is not concave, implying thus that multiple local optima may exist; *iii*) a feasible solution may not occur, since there may not be a TPs combination that simultaneously satisfies all the constraints; *iv*) the "no-solution" condition could be pragmatically relaxed by dropping the packets violating the constraints, or even blocking the corresponding users for a given time interval. Concluding, an affordable numerical algorithm is called for, which will be the focus of the next two sections.

IV. Iterative Solution of the MMG-OP

The rationale to solve the MMG-OP introduced in Sect. III-B relies on the "divide et impera" concept, i.e., subdividing the main problem into the AMC, PA and SA subproblems, and then, efficiently solving each of them. Specifically, in Sect. IV-A, the solving algorithm of the MMG-OP based on the CAM procedure has been formalized. In Sect. IV-B and IV-C, we tackle the solution of the AMC- and PA-OP, respectively, while Sect. V deals with the SA-OP. In the sequel, for notational simplicity, we will further drop the dependence of the quantities of interest on the CSI $\mathbf{h}$, that is assumed to be known to the transmitter at each PR.

A. Outline of the Solution Algorithm to the MMG-OP

The search for a solution to the MMG-OP is based on the CAM algorithm [25]. The rationale consists in iteratively optimizing the objective function $\xi(\boldsymbol{\tau})$ w.r.t. only a subset $\mathbf{y}$ of the TPs, while keeping the remaining ones, identified as $\boldsymbol{\tau}_{-\mathbf{y}}$, fixed to the values found at the previous iteration. Denoting with $\mathbf{a}^{(i)} \triangleq [{\mathbf{a}_1^{(i)}}^T, \cdots, {\mathbf{a}_Q^{(i)}}^T]^T$, $\mathbf{m}^{(i)} \triangleq [m_1^{(i)}, \cdots, m_Q^{(i)}]^T$, and $\mathbf{r}^{(i)} \triangleq [r_1^{(i)}, \cdots, r_Q^{(i)}]^T$ the SA, bit and coding rate vectors at the ith iteration, respectively, and assuming that the three subproblems are tackled according to a given succession, the MMG-OP is solved by the pseudo-code illustrated in Tab. I, returning:

i) for the AMC-OP, $\{\mathbf{m}^{(i+1)}, \mathbf{r}^{(i+1)}\}$, given $\boldsymbol{\tau}_{-\{\mathbf{m},\mathbf{r}\}}^{(i)} \triangleq \{\mathbf{p}^{(i)}, \mathbf{a}^{(i)}\}$;

ii) for the PA-OP, $\mathbf{p}^{(i+1)}$, given $\boldsymbol{\tau}_{-\mathbf{p}}^{(i)} \triangleq \{\mathbf{a}^{(i)}, \mathbf{m}^{(i+1)}, \mathbf{r}^{(i+1)}\}$;

iii) for the SA-OP, $\mathbf{a}^{(i+1)}$, given $\boldsymbol{\tau}_{-\mathbf{a}}^{(i)} \triangleq \{\mathbf{p}^{(i+1)}, \mathbf{m}^{(i+1)}, \mathbf{r}^{(i+1)}\}$.

The following features can be pointed out: *i*) since the AMC-, PA- and SA-OP are optimally solved, each iteration yields a nondecreasing value of the objective function; *ii*) the algorithm ends when either it converges to a local optimum within the accuracy interval ϵ or reaches the maximum number of iterations I_{CAM}, returning in both cases the solution $\boldsymbol{\tau}^\star$; *iii*) in order to improve the chances to converge to a "good" local optimum among all possible ones, the algorithm has to be properly initialized by finding a suitable $\boldsymbol{\tau}^{(0)}$ and the three subproblems must be solved according the best performing succession, as shown in Sect. VI; *iv*) the overall computational complexity is linear in I_{CAM}, whereas the complexity of a single iteration is given by that of the algorithms solving the three subproblems, as discussed at the end of their relevant sections. From now on, for notational simplicity, we will drop w.l.g. the dependence of iteration index i of the CAM algorithm from the quantities of interest.

B. Solution to the AMC-OP

The AMC-OP, which is solved by the optimal bit and coding rate vectors $\{\mathbf{m}^\star, \mathbf{r}^\star\}$, with $\mathbf{m}^\star \triangleq [m_1^\star, \cdots, m_Q^\star]^T$ and $\mathbf{r}^\star \triangleq [r_1^\star, \cdots, r_Q^\star]^T$, can be stated as follows.

Definition 2 (AMC-OP): Given $\boldsymbol{\tau}_{-\{\mathbf{m},\mathbf{r}\}}$, the MMG-OP (4) reduces to

$$\begin{aligned} \{\mathbf{m}^\star, \mathbf{r}^\star\} \quad &= \quad \underset{\{\mathbf{m},\mathbf{r}\} \in \mathcal{D}_{\mathrm{m}}^Q \times \mathcal{D}_{\mathrm{r}}^Q}{\arg\max} \; \xi(\mathbf{m}, \mathbf{r}) \\ \text{s.t.} \quad & \quad \Phi_{r_q}\left[\bar{\gamma}_q(m_q)\right] \leq \Upsilon_q, \qquad \forall q \in \mathcal{Q}. \quad \text{(a)} \end{aligned} \tag{7}$$

Given the finite cardinality of the domain $\mathcal{D}_{\mathrm{mr}} \triangleq \mathcal{D}_{\mathrm{m}} \times \mathcal{D}_{\mathrm{r}}$, the AMC-OP[6] is solved through the "worst case" exhaustive method summarized in Tab. II. Each iteration checks if there exists a pair of modulation and coding format that increases the lowest EGP while satisfying the QoS constraint (7.a). Iterations go on until the user with the worst EGP cannot improve its performance anymore, thus concluding the search. Concerning the complexity of the solution to the AMC-OP, it can be verified that it is linear in the size $|\mathcal{D}_{\mathrm{mr}}|$ times the required number of iterations, which in turn (from simulation results not shown due limitation of pages) shows at most

[6]Concerning the choice of adopting uniform bit loading (BL) for each user, we observe that the assumption can be removed by applying, for instance, the efficient BL algorithm proposed in [32] without modifying the proposed CAM-based approach. Hence, since this topic does not add any additional novelty, in the current work we will focus on uniform BL only.

CAM-based solution algorithm to the MMG-OP
Input: ϵ, I_{CAM}, $\boldsymbol{\tau}_0$
Initialize: $i = 0$, $\boldsymbol{\tau}^{(0)} = \boldsymbol{\tau}_0$
Repeat
Solve AMC-OP: $\{\mathbf{m}^{(i+1)}, \mathbf{r}^{(i+1)}\} = \underset{\{\mathbf{m},\mathbf{r}\} \in \mathcal{D}_{\mathrm{m}}^Q \times \mathcal{D}_{\mathrm{r}}^Q}{\arg\max} \xi(\mathbf{m}, \mathbf{r} \,|\, \boldsymbol{\tau}_{-\{\mathbf{m},\mathbf{r}\}}^{(i)})$
Solve PA-OP: $\mathbf{p}^{(i+1)} = \underset{\mathbf{p} \in \mathcal{D}_{\mathrm{p}}^N}{\arg\max}\, \xi(\mathbf{p} \,|\, \boldsymbol{\tau}_{-\mathbf{p}}^{(i)})$
Solve SA-OP: $\mathbf{a}^{(i+1)} = \underset{\mathbf{a} \in \mathcal{D}_{\mathrm{a}}^{NQ}}{\arg\max}\, \xi(\mathbf{a} \,|\, \boldsymbol{\tau}_{-\mathbf{a}}^{(i)})$
Set $i = i + 1$
Update $\boldsymbol{\tau}^{(i)}$ **with** $\{\mathbf{p}^{(i)}, \mathbf{a}^{(i)}, \mathbf{m}^{(i)}, \mathbf{r}^{(i)}\}$
Until $\left\|\xi(\boldsymbol{\tau}^{(i)}) - \xi(\boldsymbol{\tau}^{(i-1)})\right\| < \epsilon$ **Or** $i = I_{\mathrm{CAM}}$
Output: $\boldsymbol{\tau}^\star = \boldsymbol{\tau}^{(i)}$

TABLE I

the same order of magnitude of the number of users besides scaling with it.

C. Solution to the PA-OP

The PA-OP returning the optimal power distribution $\mathbf{p}^\star \triangleq [p_1^\star, \cdots, p_N^\star]^T$ across the N subcarriers can be formulated as follows.

Proposition 1 (PA-OP): Given $\boldsymbol{\tau}_{-\mathbf{p}}$ and defining from (4.c) $\upsilon_q \triangleq \Phi_{r_q}^{-1}(\Upsilon_q)$, $\forall q \in \mathcal{Q}$, the MMG-OP can be rearranged into the convex OP

$$\begin{aligned} \min_{t,\, \mathbf{p}\in\mathcal{D}_{\mathrm{p}}^N} \quad & -t \\ \text{s.t.} \quad & \textstyle\sum_{n\in\mathcal{N}} p_n - P \leq 0, && \text{(a)} \\ & t - \zeta_q(\mathbf{p}) \leq 0, \qquad \forall q \in \mathcal{Q}, && \text{(b)} \\ & \upsilon_q - \overline{\gamma}_q(\mathbf{p}) \leq 0, \qquad \forall q \in \mathcal{Q}. && \text{(c)} \end{aligned} \tag{8}$$

Proof: Exploiting (3), for a given $\boldsymbol{\tau}_{-\mathbf{p}}$, the normalized EGP in (6) results as $\zeta_q(\mathbf{p})/\zeta_q^{(0)} = 1 - \Phi_{r_q}\{-\log[z(\mathbf{p})]\}$, where $z(\mathbf{p}) \triangleq \frac{1}{\Omega_q^{(0)}} \sum_{n\in\mathcal{N}} a_{q,n}\Omega_{q,n}(p_n)$, with $\zeta_q^{(0)} \triangleq \frac{N_q^{(\mathrm{p})}}{N_q^{(\mathrm{u})}} r_q\, m_q \sum_{n\in\mathcal{N}} a_{q,n}$ and $\Omega_q^{(0)} \triangleq m_q \sum_{n\in\mathcal{N}} a_{q,n}$ depending on $\boldsymbol{\tau}_{-\mathbf{p}}$ only. Since *i*) both $-\log(\cdot)$ and $\Phi_{r_q}(\cdot)$ are convex and non-increasing functions, and *ii*) $z(\mathbf{p})$ is convex according to the expression of $\Omega_{q,n}(p_n)$, due to the composition rule of convexity [26], it can be argued that $\zeta_q(\mathbf{p})$ is a concave function of $\mathbf{p}$. Thus, the objective function (5) is concave as well, being the minimum among a set of concave functions. Upon observing that, given $\boldsymbol{\tau}_{-\mathbf{p}}$, the $\mathbf{p}$-dependent constraints (4.a) and (4.c) are convex, the maximization of (5) over a convex set results as a convex OP. Therefore, as shown in [12], the PA-OP can be equivalently reformulated into its epigraph form (8). ■

In view of the nonlinear nature of (8), the optimal solution $\mathbf{p}^\star$ can be found applying the LDD theory [26], i.e., by solving the dual OP associated to the primal problem (8), as illustrated in the following proposition.

Proposition 2 (Solution to the PA-OP based on the LDD): Let us introduce the Lagrangian multipliers θ, ω_q and ϕ_q, $\forall q \in \mathcal{Q}$, associated to the constrains (8.a), (8.b) and (8.c), respectively. Then, after stacking them into the $(2Q+1)$-sized vector $\boldsymbol{\Theta} \triangleq [\theta, \omega_1, \cdots, \omega_Q, \phi_1, \cdots, \phi_Q]^T$ and defining $\mathbf{d}(\mathbf{p}) \triangleq \big[\sum_{n\in\mathcal{N}} p_n - P, -\zeta_1(\mathbf{p}), \cdots, -\zeta_Q(\mathbf{p}), \upsilon_1 - \overline{\gamma}_1(\mathbf{p}), \cdots, \upsilon_Q - \overline{\gamma}_Q(\mathbf{p})\big]^T$, the dual function of the PA-OP (8) results as

$$g(\boldsymbol{\Theta}) = \inf_{\mathbf{p}\in\mathcal{D}_{\mathrm{p}}^N} \{\boldsymbol{\Theta}^T \mathbf{d}(\mathbf{p})\}, \tag{9}$$

where the feasible set for the dual variables $\boldsymbol{\Theta}$ is defined as $\mathcal{D}_{\boldsymbol{\Theta}} \triangleq \mathcal{D}_\theta \times \mathcal{D}_\phi^Q \times [\mathcal{D}_\omega^Q \cap \mathcal{D}_{\bar{\omega}}]$, with $\mathcal{D}_\theta \triangleq \{\theta \in \mathbb{R} \,|\, \theta \geq 0,\}$, $\mathcal{D}_\phi \triangleq \{\phi_q \in \mathbb{R} \,|\, \phi_q \geq 0, \forall q \in \mathcal{Q}\}$, $\mathcal{D}_\omega \triangleq \{\omega_q \in \mathbb{R} \,|\, \omega_q \geq 0, \forall q \in \mathcal{Q}\}$, and $\mathcal{D}_{\bar{\omega}} \triangleq \{\omega_q \in \mathbb{R} \,|\, \sum_{q\in\mathcal{Q}} \omega_q = 1\}$. The optimal $\boldsymbol{\Theta}^\star$ is thus obtained by solving the dual OP

$$\boldsymbol{\Theta}^\star = \arg\max_{\boldsymbol{\Theta}\in\mathcal{D}_{\boldsymbol{\Theta}}} g(\boldsymbol{\Theta}), \tag{10}$$

and consequently, the optimal solution of the primal OP results as $\mathbf{p}^\star = \mathbf{p}(\boldsymbol{\Theta}^\star)$, $\mathbf{p}(\boldsymbol{\Theta})$ being the optimal solution to (9) for a given $\boldsymbol{\Theta}$.

Proof: Since the objective function and constraints in (8) are continuously differentiable and convex, the Karush-Kuhn-Tucker (KKT) conditions are necessary and sufficient for primal-dual optimality [26]. Therefore, strong duality exists, i.e., the difference between the optimal primal and dual objectives (duality gap) is zero. From (8), the dual function can be written as

$$G(\boldsymbol{\Theta}) \triangleq \inf_{\mathbf{p}\in\mathcal{D}_{\mathrm{p}}^N, t} \left\{ \left(\sum_{q\in\mathcal{Q}} \omega_q - 1 \right) \cdot t + \boldsymbol{\Theta}^T \mathbf{d}(\mathbf{p}) \right\}. \tag{11}$$

Since the infimum of t is $-\infty$ unless it is multiplied by an identically null coefficient, then $\sum_{q\in\mathcal{Q}} \omega_q - 1 = 0$ follows, and so, the dual function turns into (9), where the dual variables $\boldsymbol{\Theta}$ belong to the feasible set $\mathcal{D}_{\boldsymbol{\Theta}}$ defined above. Hence, solving the dual OP (10) provides the optimal $\boldsymbol{\Theta}^\star$, and in view of the strong duality, also the optimal solution $\mathbf{p}^\star = \mathbf{p}(\boldsymbol{\Theta}^\star)$ of the original PA-OP, where $\mathbf{p}(\boldsymbol{\Theta}) \triangleq \arg\min_{\mathbf{p}\in\mathcal{D}_{\mathrm{p}}^N} \{\boldsymbol{\Theta}^T \mathbf{d}(\mathbf{p})\}$. ■

The numerical procedure to solve the PA-OP is summarized in Tab. III, where ϵ, $I_{\max}$ and $\boldsymbol{\Theta}_0$ denote the desired accuracy, the maximum number of iterations and the initialization value for $\boldsymbol{\Theta}$, respectively. About this LDD-based approach, it can be remarked that: *i*) due to the convexity of the PA-OP, any local optimum is globally optimal as well; *ii*) the proposed method has a worst case convergence of $\mathcal{O}(1/\epsilon^2)$ [33]; *iii*) since the solution $\boldsymbol{\Theta}^\star$ to (10) does not exist in closed-form, a viable algorithm consists in iteratively updating $\boldsymbol{\Theta}$ via the sub-gradient algorithm with step-size δ [25] (see Appendix B for further details), whereas the search for $\mathbf{p}(\boldsymbol{\Theta})$ can be performed via conventional optimization algorithms like the steepest descent or the ellipsoid methods [26].

Solution algorithm to the AMC-OP

Input: $\boldsymbol{\tau}_{-\{\mathbf{m},\mathbf{r}\}}$, $\{\mathbf{m}_0, \mathbf{r}_0\}$
Initialize: $k = 1$, $u^{(0)} = 0$, $\boldsymbol{\tau} = \boldsymbol{\tau}_{-\{\mathbf{m},\mathbf{r}\}}$, $\{\mathbf{m}, \mathbf{r}\} = \{\mathbf{m}_0, \mathbf{r}_0\}$
Start: Set $u^{(k)} = \arg\min_{q\in\mathcal{Q}} \zeta_q(m_q, r_q)$, $\overline{\mathcal{Q}} = \mathcal{Q}\backslash\{u^{(k)}\}$
If $u^{(k)} \neq u^{(k-1)}$
  For $i = 1 : |\mathcal{D}_{\mathrm{mr}}|$
    If $\zeta_{u^{(k)}}(\mathcal{D}_{\mathrm{mr}}(i)) > \zeta_{u^{(k)}}(m_{u^{(k)}}, r_{u^{(k)}})$ **And** (7.a) **holds**
      Set $\{m_{u^{(k)}}, r_{u^{(k)}}\} = \mathcal{D}_{\mathrm{mr}}(i)$
      If $\zeta_{u^{(k)}}(\mathcal{D}_{\mathrm{mr}}(i)) > \min_{q\in\overline{\mathcal{Q}}} \{\zeta_q(m_q, r_q)\}$
        Set $k = k + 1$
        Go to Start:
      End If
    End If
  End For
End if
Output: $\{\mathbf{m}^\star, \mathbf{r}^\star\} = \{\mathbf{m}, \mathbf{r}\}$

TABLE II

V. Solution to the SA-OP

Herein, we focus on the solution to the SA-OP, which is by far the most demanding one when compared with the solution algorithms to the AMC-OP and PA-OP discussed in Sects. IV-B and IV-C, respectively.

Solution algorithm to the PA-OP
Input: δ, ϵ, $I_{\max}$, $\boldsymbol{\tau}_{-\mathbf{p}}$, $\boldsymbol{\Theta}_0$
Initialize: $i=0$, $\boldsymbol{\tau}=\boldsymbol{\tau}_{-\mathbf{p}}$, $\boldsymbol{\Theta}^{(0)}=\boldsymbol{\Theta}_0$
Repeat
$\mathbf{p}(\boldsymbol{\Theta}^{(i)})=\arg\min_{\mathbf{p}\in\mathcal{D}_{\mathrm{p}}^{N}}\{\boldsymbol{\Theta}^{(i)T}\mathbf{d}(\mathbf{p})\}$
$\boldsymbol{\Theta}^{(i+1)}=\left[\boldsymbol{\Theta}^{(i)}+\delta\nabla_{\boldsymbol{\Theta}}g(\boldsymbol{\Theta}^{(i)})\right]_{\mathcal{D}_{\boldsymbol{\Theta}}}$
Set $i=i+1$
Until $\left\|\mathbf{p}(\boldsymbol{\Theta}^{(i)})-\mathbf{p}(\boldsymbol{\Theta}^{(i-1)})\right\|<\epsilon$ **Or** $i=I_{\max}$
Output: $\mathbf{p}^{\star}=\mathbf{p}(\boldsymbol{\Theta}^{(i)})$

TABLE III

A. Formulation of the SA-OP and Outline of the Solution Algorithm

The SA-OP, whose solution consists of the SA vector $\mathbf{a}^{\star}\triangleq[\mathbf{a}_1^{\star T},\cdots,\mathbf{a}_Q^{\star T}]^T$, with $\mathbf{a}_q^{\star}\triangleq[a_{q,1}^{\star},\cdots,a_{q,N}^{\star}]^T$, $\forall q\in\mathcal{Q}$, can be defined by the following proposition.

Definition 3 (SA-OP): Given $\boldsymbol{\tau}_{-\mathbf{a}}$, the MMG-OP (4) turns out

$$\begin{aligned}\mathbf{a}^{\star}=\ & \underset{\mathbf{a}\in\mathcal{D}_{\mathrm{a}}^{NQ}}{\arg\max}\ \left\{\min_{q\in\mathcal{Q}}\zeta_q(\mathbf{a}_q)\right\}\\ \text{s.t.}\ & \textstyle\sum_{q\in\mathcal{Q}}a_{q,n}\le 1, && \forall n\in\mathcal{N},\quad \text{(a)}\\ & \overline{\gamma}_q(\mathbf{a}_q)\ge\upsilon_q, && \forall q\in\mathcal{Q}.\quad \text{(b)}\end{aligned}\tag{12}$$

From (12), it is apparent that the SA-OP is an NP-hard nonlinear IP problem with NQ binary optimization variables, i.e., the entries of $\mathbf{a}\triangleq[\mathbf{a}_1^T,\cdots,\mathbf{a}_Q^T]^T\in\mathcal{D}_{\mathrm{a}}^{NQ}$. In light of the extreme difficulty involved in searching for the optimal solution $\mathbf{a}^{\star}$, two different approaches are proposed as follows.

1) Relaxed SA-OP combined with the B&B algorithm.
   1.a) In Sect. V-B.1, the SA-OP is converted in its *relaxed* version, termed RSA-OP, where the binary optimization variables $a_{q,n}\in\mathcal{D}_{\mathrm{a}}$ are replaced by the continuous ones $\breve{a}_{q,n}\in\mathcal{D}_{\breve{\mathrm{a}}}\triangleq\{\breve{a}_{q,n}\in\mathbb{R}\,|\,\breve{a}_{q,n}\in[0,1],\forall n\in\mathcal{N},\forall q\in\mathcal{Q}\}$. Accordingly, $\breve{\mathbf{a}}\triangleq[\breve{\mathbf{a}}_1^T,\cdots,\breve{\mathbf{a}}_Q^T]^T\in\mathcal{D}_{\breve{\mathrm{a}}}^{NQ}$ and $\breve{\mathbf{a}}_q\triangleq[\breve{a}_{q,1},\cdots,\breve{a}_{q,N}]^T\in\mathcal{D}_{\breve{\mathrm{a}}}^{N}$, $\forall q\in\mathcal{Q}$, take the place of $\mathbf{a}\in\mathcal{D}_{\mathrm{a}}^{NQ}$ and $\mathbf{a}_q\in\mathcal{D}_{\mathrm{a}}^{N}$, respectively. Interesting to note, despite its apparently harsh structure, it will be proved that the the RSA-OP is a convex OP, whose solution yields an upper bound (UB) for the optimal value of the objective function in (12).
   1.b) The optimal solution of the SA-OP (12) is then obtained in Sect. V-B.2 by mapping the relaxed solution of the RSA-OP back to the original discrete domain $\mathcal{D}_{\mathrm{a}}^{NQ}$ via the B&B algorithm [27].
2) ACO-based SA-OP.
   In Sect. V-C, an alternative yet more affordable method to solve (12) is formulated exploiting the ACO framework, which enables an efficient accuracy-versus-complexity tradeoff.

B. Relaxed SA-OP Combined with the B&B Algorithm

1. The relaxed SA-OP

In order to obtain the relaxed version of the SA-OP, let us reformulate the EGP of user q in (2) by substituting $a_{q,n}\in\mathcal{D}_{\mathrm{a}}$ with $\breve{a}_{q,n}\in\mathcal{D}_{\breve{\mathrm{a}}}$, thus obtaining

$$\zeta_q(\breve{\mathbf{a}}_q)=\varsigma_q\sum_{n\in\mathcal{N}}\breve{a}_{q,n}\left[1-\Psi_q\left(\frac{1}{m_q}\cdot\frac{\sum_{n\in\mathcal{N}}\Omega_{q,n}\breve{a}_{q,n}}{\sum_{i\in\mathcal{N}}\breve{a}_{q,i}}\right)\right],\tag{13}$$

where $\varsigma_q\triangleq N_q^{(\mathrm{p})}r_q m_q/N_q^{(\mathrm{u})}$ and $\Psi_q\triangleq\Phi_{r_q}\circ(-\log)$. Note that the continuous variables $\breve{a}_{q,n}$ play in: *i*) two *unweighed* sums, one multiplying the content of the square brackets and the other at the denominator of the argument of Ψ_q; *ii*) a *weighed* sum at the numerator of the argument of Ψ_q. Such remarks pave the way to the following proposition.

Proposition 3 (LB of the EGP and Related Properties): Upon defining the slack variables $s_q>0$, $\forall q\in\mathcal{Q}$, the (non-strict) inequality

$$\begin{aligned}\tilde{\zeta}_q(\breve{\mathbf{a}}_q,s_q)\triangleq\ & \varsigma_q s_q\left[1-\Psi_q\left(\frac{1}{m_q}\cdot\frac{\sum_{n\in\mathcal{N}}\Omega_{q,n}\breve{a}_{q,n}}{s_q}\right)\right]\\ & \le\zeta_q(\breve{\mathbf{a}}_q)\end{aligned}\tag{14}$$

holds whenever

$$s_q\le\sum_{n\in\mathcal{N}}\breve{a}_{q,n},\tag{15}$$

with the following properties:
P1) $\tilde{\zeta}_q(\breve{\mathbf{a}}_q,s_q)$ is a monotone nondecreasing function of s_q;
P2) $\tilde{\zeta}_q(\breve{\mathbf{a}}_q,s_q)$ under constraint (15) defines a LB of $\zeta_q(\breve{\mathbf{a}}_q)$ in the continuous domain;
P3) when $s_q=\sum_{n\in\mathcal{N}}\breve{a}_{q,n}$, (14) holds with the equality, i.e., $\tilde{\zeta}_q(\breve{\mathbf{a}}_q,s_q)=\zeta_q(\breve{\mathbf{a}}_q)$;
P4) $\tilde{\zeta}_q(\breve{\mathbf{a}}_q,s_q)$ is *jointly concave* w.r.t. $(\breve{\mathbf{a}}_q,s_q)$;
P5) maximizing $\min_{q\in\mathcal{Q}}\{\tilde{\zeta}_q(\breve{\mathbf{a}}_q,s_q)\}$ over $\breve{\mathbf{a}}$ and s_q, $q\in\mathcal{Q}$, yields a unique optimal SA solution that coincides with the one that also maximizes $\min_{q\in\mathcal{Q}}\{\zeta_q(\breve{\mathbf{a}}_q)\}$ over $\breve{\mathbf{a}}$.

Proof: Given $\breve{\mathbf{a}}_q$, P1 is easily proved by evaluating the sign of the first order derivative of $\tilde{\zeta}_q(\breve{\mathbf{a}}_q,s_q)$ w.r.t. s_q, while P2 and P3 directly follow from (15).

Concerning P4, let us first observe that $\overline{\Psi}_q(\breve{\mathbf{a}}_q)\triangleq 1-\Psi_q(\frac{1}{m_q}\sum_{n\in\mathcal{N}}\Omega_{q,n}\breve{a}_{q,n})$ is concave in $\breve{\mathbf{a}}_q$, in that the function composition Ψ_q is convex due to the rule of composition of convex functions [26]. Then, since $s_q>0$, it comes out that $\tilde{\zeta}_q(\breve{\mathbf{a}}_q,s_q)=\varsigma_q s_q\overline{\Psi}_q(\breve{\mathbf{a}}_q/s_q)$ (up to the immaterial factor ς_q) is the perspective function of $\overline{\Psi}_q(\breve{\mathbf{a}}_q)$. As a consequence, since the perspective of a concave function is still concave [27], P4 follows.

As for P5, denoting with $\bar{q}\triangleq\arg\min_{q\in\mathcal{Q}}\{\tilde{\zeta}_q(\breve{\mathbf{a}}_q,s_q)\}$ and $\mathcal{D}_{\mathrm{s}}\triangleq\{s_q\in\mathbb{R}^{+}\,|\,s_q\le\sum_{n\in\mathcal{N}}\breve{a}_{q,n},\forall q\in\mathcal{Q}\}$, then $\max_{\breve{\mathbf{a}}_{\bar{q}}\in\mathcal{D}_{\breve{\mathrm{a}}}^{N},\,s_{\bar{q}}\in\mathcal{D}_{\mathrm{s}}}\{\tilde{\zeta}_{\bar{q}}(\breve{\mathbf{a}}_{\bar{q}},s_{\bar{q}})\}=\tilde{\zeta}_{\bar{q}}(\breve{\mathbf{a}}_{\bar{q}}^{\star},s_{\bar{q}}^{\star})$, since there exists an unique optimal solution due to P4, with $s_{\bar{q}}^{\star}=\sum_{n\in\mathcal{N}}\breve{a}_{\bar{q},n}^{\star}$ due to P1. Thus, exploiting P3 yields $\tilde{\zeta}_{\bar{q}}(\breve{\mathbf{a}}_{\bar{q}}^{\star},\sum_{n\in\mathcal{N}}\breve{a}_{\bar{q},n}^{\star})=\zeta_{\bar{q}}(\breve{\mathbf{a}}_{\bar{q}}^{\star})$, and eventually, $\max_{\breve{\mathbf{a}}_{\bar{q}}\in\mathcal{D}_{\breve{\mathrm{a}}}^{N},\,s_{\bar{q}}\in\mathcal{D}_{\mathrm{s}}}\{\tilde{\zeta}_{\bar{q}}(\breve{\mathbf{a}}_{\bar{q}},s_{\bar{q}})\}=\max_{\breve{\mathbf{a}}_{\bar{q}}\in\mathcal{D}_{\breve{\mathrm{a}}}^{N}}\{\zeta_{\bar{q}}(\breve{\mathbf{a}}_{\bar{q}})\}$. ■

The above results lead to the formulation of the RSA-OP.

Definition 4 (RSA-OP): Given $\boldsymbol{\tau}_{-\mathbf{a}}$ and assuming $\breve{\mathbf{a}} \in \mathcal{D}_{\breve{\mathrm{a}}}^{NQ}$ along with $\mathbf{s} \triangleq [s_1, \cdots, s_Q]^T$ as optimization variables, the RSA-OP can be written as

$$\begin{aligned} \{\breve{\mathbf{a}}^\star, \mathbf{s}^\star\} = & \underset{\breve{\mathbf{a}} \in \mathcal{D}_{\breve{\mathrm{a}}}^{NQ}, \mathbf{s}}{\arg\max} \ \{\min_{q \in \mathcal{Q}} \tilde{\zeta}_q(\breve{\mathbf{a}}_q, s_q)\} \\ \text{s.t.} \quad & \textstyle\sum_{q \in \mathcal{Q}} \breve{a}_{q,n} \leq 1, \forall n \in \mathcal{N}, & \text{(a)} \\ & s_q - \textstyle\sum_{n \in \mathcal{N}} \breve{a}_{q,n} \leq 0, \forall q \in \mathcal{Q}, & \text{(b)} \\ & \textstyle\sum_{n \in \mathcal{N}} (\Omega_{q,n} - m_q \mathrm{e}^{-\upsilon_q}) \breve{a}_{q,n} \leq 0, \forall q \in \mathcal{Q}, & \text{(c)} \end{aligned} \tag{16}$$

where $\breve{\mathbf{a}}^\star \triangleq [\breve{\mathbf{a}}_1^{\star T}, \cdots, \breve{\mathbf{a}}_Q^{\star T}]^T$ with $\breve{\mathbf{a}}_q^\star \triangleq [\breve{a}_{q,1}^\star, \cdots, \breve{a}_{q,N}^\star]^T$, $\mathbf{s}^\star \triangleq [s_1^\star, \cdots, s_Q^\star]^T$, (16.c) corresponds to the constraint (4.c) expressed as a function of the elements of $\breve{\mathbf{a}}_q$, with $\upsilon_q = \Phi_{r_q}^{-1}(\Upsilon_q)$, $q \in \mathcal{Q}$, as defined at the beginning of Sec. IV-C.

The problem we are left now is how to find the optimal solution $\breve{\mathbf{a}}^\star$ solving (16). Bearing in mind that the objective function is jointly concave w.r.t. $(\breve{\mathbf{a}}_q, s_q)$ (property P4), a CAM-based algorithm can be applied running iteratively between the two concave subproblems RSA-OP.1 and RSA-OP.2, as summarized in Tab. V-B. As for RSA-OP.1, given $\breve{\mathbf{a}}_q$, $\tilde{\zeta}_q(\breve{\mathbf{a}}_q, s_q)$ is a monotonically nondecreasing function of s_q (property P1), and therefore, the optimal solution at iteration $(j+1)$ is simply $s_q^{(j+1)} = \sum_{n \in \mathcal{N}} \breve{a}_{q,n}^{(j)}$. The subproblem RSA-OP.2, instead, can be solved applying the LDD method, similarly to what done for the PA-OP in Sect. IV-C. In view of the properties P1-P5, it is guaranteed that the proposed numerical procedure to solve the RSA-OP converges to the global optimum [25], whereas its overall complexity is given by that of the LDD solution to the RSA-OP.2 times the number of required iterations.

2. The B&B-based solution to the SA-OP

The next (and final) step to solve the SA-OP consists in starting from the solution $\breve{\mathbf{a}}^\star$ to the RSA-OP over the continuous domain $\mathcal{D}_{\breve{\mathrm{a}}}^{NQ}$ and coming back to the solution $\mathbf{a}^\star$ in the original discrete domain $\mathcal{D}_{\mathrm{a}}^{NQ}$ by means of the B&B algorithm. Exploiting the fact that $\breve{\mathbf{a}}^\star$ provides an UB for the optimal value of the objective function in (12) (since the optimization is made over the larger set $\mathcal{D}_{\breve{\mathrm{a}}}^{NQ}$), the B&B-based search algorithm relies on iteratively building a graph, each node of which is associated to:

- a set $\mathcal{A} \subset \mathcal{D}_{\breve{\mathrm{a}}}^{NQ}$, whose elements, say $\breve{\mathbf{a}}$, are the possible intermediate solutions to the SA-OP having entries $\breve{a}_{q,n}$, that can be either quantized to $\{0,1\}$ or continuous variables in $[0,1]$;
- the UB $\xi_{\mathrm{UB}}(\mathcal{A})$ of the optimal value $\xi^\star$ of the EGP given by (5), found by solving the RSA-OP when adopting $\breve{\mathbf{a}} \in \mathcal{A}$;
- the LB $\xi_{\mathrm{LB}}(\mathcal{A})$ of $\xi^\star$, obtained by rounding to the nearest integer the entries of the solution of the UB problem.

Let us give a brief outline about how the B&B can be applied; for additional details see [27]. Denote with $\mathcal{I}_k$ the set collecting the sets $\mathcal{A}_k$ associated to all the nodes at iteration k, and with U_k and L_k the best UB and LB, respectively, found till then. The graph begins with a single node corresponding to $\mathcal{I}_0 = \{\mathcal{D}_{\breve{\mathrm{a}}}^{NQ}\}$, meaning that all the NQ subcarrier indexes are allowed to take continuous values in $[0,1]$. The generic kth iteration, $k \geq 1$, is made up of the following four steps.

S1) *Branching*. The set $\bar{\mathcal{A}} \in \mathcal{I}_k$ is chosen as the one having the lowest UB $\xi_{\mathrm{UB}}(\bar{\mathcal{A}})$. Then, two child nodes, say $\bar{\mathcal{A}}_1$ and $\bar{\mathcal{A}}_0$, are generated from $\bar{\mathcal{A}}$ according to the following rule: for $\bar{\mathcal{A}}_1$, the continuous variable $\breve{a}_{\bar{q},\bar{n}}$, $\bar{q} \in \mathcal{Q}$ and $\bar{n} \in \mathcal{N}$, taking the value closest to $1/2$ is set to 1, while due to the OFDMA orthogonality principle, $\breve{a}_{q,\bar{n}}$, $\forall q \in \mathcal{Q}$ with $q \neq \bar{q}$, are replaced with 0; for $\bar{\mathcal{A}}_0$, we set $\breve{a}_{\bar{q},\bar{n}} = 0$. Correspondingly, $\mathcal{I}_{k+1}$ is built by removing $\bar{\mathcal{A}}$ from $\mathcal{I}_k$ and adding $\bar{\mathcal{A}}_0$ and $\bar{\mathcal{A}}_1$ into the updated set.

S2) *Bounding*. The UBs and LBs for $\bar{\mathcal{A}}_0$ and $\bar{\mathcal{A}}_1$ are evaluated, and then, the best bounds are updated as $U_{k+1} = \min\{U_k, \xi_{\mathrm{UB}}(\bar{\mathcal{A}}_0), \xi_{\mathrm{UB}}(\bar{\mathcal{A}}_1)\}$ and $L_{k+1} = \min\{L_k, \xi_{\mathrm{LB}}(\bar{\mathcal{A}}_0), \xi_{\mathrm{LB}}(\bar{\mathcal{A}}_1)\}$.

S3) *Pruning*. The sets $\mathcal{A} \in \mathcal{I}_{k+1}$ such that $\xi_{\mathrm{UB}}(\mathcal{A}) < L_{k+1}$ are pruned, i.e., they are removed from $\mathcal{I}_{k+1}$ along with the corresponding nodes.

S4) *Testing*. When the condition $U_{k+1} - L_{k+1} < \epsilon$ holds, with ϵ denoting the chosen accuracy, the algorithm stops and returns the discrete optimal solution $\mathbf{a}^\star \in \mathcal{D}_{\mathrm{a}}^{NQ}$, i.e., the one associated to the LB; otherwise, the procedure goes on with the next iteration starting from S1.

Some remarks are of interest about the solution to the SA-OP based on the RSA-OP combined with the B&B algorithm: *i*) the B&B algorithm exhibits a worst-case complexity equalling that of the demanding exhaustive search over all the graph nodes; *ii*) at each node, in order to get the UB, the RSA-OP has to be solved applying the iterative LDD method; *iii*) although the B&B-based solution is ϵ-optimal, as a matter of fact the price to be paid is a prohibitive complexity, and as such, in the following, it will be taken as a *performance benchmark* only.

CAM-based algorithm for the RSA-OP

Input: ϵ, J_{CAM}, $\boldsymbol{\tau}_{-\mathbf{a}}$, $\breve{\mathbf{a}}_0$
Initialize: $j = 0$, $\boldsymbol{\tau} = \boldsymbol{\tau}_{-\mathbf{a}}$, $\breve{\mathbf{a}}^{(0)} = \breve{\mathbf{a}}_0$
Repeat

Solve RSA-OP.1: $\mathbf{s}^{(j+1)} = \arg\max_{\mathbf{s}} \left\{ \min_{q \in \mathcal{Q}} \tilde{\zeta}_q(\breve{\mathbf{a}}_q^{(j)}, s_q) \right\}$ s.t. (16.b)

Solve RSA-OP.2: $\breve{\mathbf{a}}^{(j+1)} = \arg\max_{\breve{\mathbf{a}} \in \mathcal{D}_{\breve{\mathrm{a}}}^{NQ}} \left\{ \min_{q \in \mathcal{Q}} \tilde{\zeta}_q(\breve{\mathbf{a}}_q, s_q^{(j+1)}) \right\}$ s.t. (16.a)-(16.c)

Set $j = j + 1$

Until $||\mathbf{s}^{(j)} - \mathbf{s}^{(j-1)}|| < \epsilon$ **Or** $j = J_{\mathrm{CAM}}$
Output: $\breve{\mathbf{a}}^\star = \breve{\mathbf{a}}^{(j)}$

C. ACO-based SA-OP

The complexity required to solve the SA-OP (12) via the method outlined in Sect. V-B actually motivates the need of formulating a more feasible numerical procedure. The key idea we pursue to achieve a computationally affordable yet accurate solution to the SA-OP relies on exploiting the metaheuristic ACO framework [28], an approach that takes inspiration from the foraging behavior of some ant species. As summarized in Appendix C, indeed, biological experiments carried out in the nineties proved that a particular substance, the *pheromone*, is deposited by the ants on the ground to mark

some favorable paths, which are then followed (preferably) by the other members of the colony, in order to search for the minimum distance from the nest to the food source. Differently from the approach taken in Sect. III-A, our aim here is to get a PER expression that can fit the ACO framework to solve the SA-OP at affordable complexity. Toward this end, let us first approximate the PER in (6) with the negative exponential $\Phi_{r_q}(\gamma) \simeq \mathrm{e}^{-\sigma_{r_q}(\gamma-\gamma_{0,r_q})}$, $\gamma \geq \gamma_{0,r_q}$, $\forall q \in \mathcal{Q}$, where the integer-valued parameters σ_{r_q} and γ_{0,r_q} are found by minimizing the mean quadratic error (MSE), taking as reference (in the range of interest for γ) the actual PER obtained by simulation of the system at hand for all the available coding rates. Then, plugging the above PER model into the EGP expression[7] (6), we obtain[8]

$$\chi_q(\mathbf{a}_q) \triangleq \underbrace{\frac{N_q^{(\mathrm{p})}}{N_q^{(\mathrm{u})}}\, r_q \left[\sum_{n\in\mathcal{N}} \Delta m_{q,n} a_{q,n}\right]}_{\lambda_q(\mathbf{a}_q)} \cdot \underbrace{\left[1 + \sum_{k=1}^{\sigma_{r_q}-1} \left(\frac{\mathrm{e}^{\gamma_{0,r_q}}}{m_q} \cdot \frac{\sum_{n\in\mathcal{N}} \Omega_{q,n} a_{q,n}}{\sum_{i\in\mathcal{N}} a_{q,i}}\right)^k\right]}_{\Lambda_q(\mathbf{a}_q)}, \forall q \in \mathcal{Q}, \quad (17)$$

where the terms $\Delta m_{q,n} \triangleq m_q - \Omega_{q,n}\mathrm{e}^{\gamma_{0,r_q}}$ are independent of the optimization variable $\mathbf{a}_q$.

The following properties can be highlighted:
P6) since $\Lambda_q(\mathbf{a}_q) \geq 1$, then $\chi_q(\mathbf{a}_q) > \lambda_q(\mathbf{a}_q)$, i.e., $\lambda_q(\mathbf{a}_q)$ is a LB of the approximate EGP (17);
P7) up to immaterial factors, $\lambda_q(\mathbf{a}_q)$ is a weighted sum of the binary-valued variables $a_{q,n}$, and so, its optimization consists in a standard integer linear programming (ILP) problem;
P8) differently from $\lambda_q(\mathbf{a}_q)$, $\Lambda_q(\mathbf{a}_q)$ is instead a nonlinear function of $\mathbf{a}_q$.

The properties P6-P8 combined with the structure of $\chi_q(\mathbf{a}_q)$ thus open the way for an effective alternative method to solve the SA-OP based on the ACO framework, heuristically handled in two steps:

1) the SA-OP-ELB, which consists in maximizing the minimum among the LBs $\lambda_q(\mathbf{a}_q)$ of the EGP, or ELBs for short, thereby returning the solution $\mathbf{a}^{\star}_{\mathrm{ELB}}$;
2) the SA-OP-ACO, where the SA-OP having (17) as objective function is solved by an iterative algorithm based on the ACO method starting from $\mathbf{a}^{\star}_{\mathrm{ELB}}$.

Definition 5 (SA-OP-ELB): The SA-OP maximizing the worst among the ELBs $\lambda_q(\mathbf{a}_q)$ can be formulated as

$$\begin{aligned} \max_{u,\, \mathbf{a}\in\mathcal{D}_{\mathrm{a}}^{NQ}} \quad & u \\ \text{s.t.} \quad & \textstyle\sum_{q\in Q} a_{q,n} \leq 1, && \forall n \in \mathcal{N}, \quad \text{(a)} \\ & \textstyle\sum_{n\in\mathcal{N}} a_{q,n}\left(\Omega_{q,n} - m_q \mathrm{e}^{-\upsilon_q}\right) \leq 0, && \forall q \in \mathcal{Q}, \quad \text{(b)} \\ & u - \lambda_q(\mathbf{a}_q) \leq 0, && \forall q \in \mathcal{Q}, \quad \text{(c)} \end{aligned} \quad (18)$$

where (18.b) is the QoS constraint (12.b) expressed in terms of the entries of $\mathbf{a}_q$.

The formulation of the ILP-OP (18) derives from both property P7 and the nature of the constraints. Its solution can therefore be found by applying conventional ILP optimization techniques [26].

Definition 6 (SA-OP-ACO): The ACO method is applied by mapping the SA-OP having the minimum of the EGP (17) as objective function onto the graph $\mathsf{G}(\mathcal{V},\mathcal{E})$ of Fig. 2, where $\mathcal{E}$ is the set of edges and $\mathcal{V}$ is the set including N vertices plus the "vertex 0", i.e., the one representing the "nest" of the ACO model.

The sets $\mathcal{E}$ and $\mathcal{V}$ are related to the SA-OP according to the following rules.
R1) The N vertices of the graph univocally represent the N subcarriers.
R2) The set of the edges $\mathcal{E} \triangleq \mathcal{E}_1 \times \cdots \times \mathcal{E}_N$, where $\mathcal{E}_n \triangleq \{e_{0,n}, e_{1,n}, \cdots, e_{Q,n}\}$, $n \in \mathcal{N}$, contains all the possible $Q+1$ edges connecting vertex $n-1$ to vertex n. Consequently, in a given path connecting vertex 0 to vertex N, the presence of the edge $e_{\bar{q},\bar{n}}$, $\bar{q} \in \mathcal{Q}$ and $\bar{n} \in \mathcal{N}$ indicates that subcarrier $\bar{n}$ is allocated to user $\bar{q}$, i.e., $a_{\bar{q},\bar{n}} = 1$ and $a_{\nu,\bar{n}} = 0$ $\forall \nu \neq \bar{q} \in \mathcal{Q}$. Conversely, the presence of $e_{0,\bar{n}}$ means that subcarrier $\bar{n}$ is unallocated, i.e., $a_{q,\bar{n}} = 0$, $\forall q \in \mathcal{Q}$.
R3) At a given iteration out of N_{it}, all the N vertices are sequentially visited by N_a virtual agents, i.e., the ants of the ACO model. Each agent independently builds a complete path by selecting, for each $n \in \mathcal{N}$, one edge among those belonging to $\mathcal{E}_n$, with probability

$$\pi_{q,n} = \frac{\eta_{q,n}\varphi_{q,n}}{\sum_{(k,n)|e_{k,n}\in\mathcal{E}_n} \eta_{k,n}\varphi_{k,n}}, \quad (19)$$

where $\eta_{i,n}$ is the *local desirability* and $\varphi_{i,n}$ the *pheromone* relevant to the generic edge $e_{i,n}$, as defined in Appendix C. Furthermore, in view of the structure of $\chi_q(\mathbf{a}_q)$ and the corresponding graph G, the quantities $\eta_{q,n}$ and $\varphi_{q,n}$, are evaluated according to the following additional rules.
R4) The local desirability is expressed as $\eta_{q,n} \triangleq [\Delta m_{q,n}]_{\bar{\eta}}^{+\infty}$, i.e., as a function of the local quantity $\Delta m_{q,n}$ depending only on the specific user q assigned to the subcarrier n. Further, $\eta_{q,n}$ is forced to be greater or equal than a suitable threshold $\bar{\eta}$, so that all the paths are guaranteed to be explored at least with a minimum (but no null) probability.
R5) The increment of the pheromone $\varphi_{q,n}$ made on the best path found at the end of the generic iteration is assumed to be proportional to Λ_q, i.e., a global quantity depending on the quality of the overall solution.

SA-OP-ACO Implementation. With reference to the pseudo-code of the SA-OP-ACO algorithm of Tab. IV, at iteration i, $1 \leq i \leq N_{\mathrm{it}}$, the path $\mathcal{T}_j^{(i)}$ built by the agent j, $1 \leq j \leq N_{\mathrm{a}}$, one-to-one identifies a possible SA vector, say $\mathbf{a}_j^{(i)}$. When iteration i is concluded, in the case the QoS constraint (18.b) is also satisfied, the algorithm releases the best value $\chi_{\mathrm{best}}^{(i)}$ of the objective function, the relevant path $\mathcal{T}_{\mathrm{best}}^{(i)}$ and solution $\mathbf{a}_{\mathrm{best}}^{(i)}$. As for the pheromone, namely, the quantity in the ACO

[7]The result $x^{i+1} = 1 - (1-x)\sum_{k=0}^{i} x^k$ has been used.
[8]For simplicity, the approximate EGP introduced in the current section, given by (17), will still be referred to as the EGP metric.

model that measures how much promising (or not) is a given solution, let remark that: *i*) on each edge, it evaporates as $\varphi_{q,n}^{(i)} \leftarrow [(1-\rho)\varphi_{q,n}^{(i-1)}]_{\varphi_{\min}}^{\varphi_{\max}}$, $\forall q \in \mathcal{Q}$, $\forall n \in \mathcal{N}$, ρ being the evaporation rate, with $0 < \rho < 1$; *ii*) in the case $\chi_{\text{best}}^{(i)} > \lambda_{\text{ELB}}^{\star}$, with $\lambda_{\text{ELB}}^{\star} \triangleq \max_{\mathbf{a}_q \in \mathcal{D}_{\text{a}}^{N}} \min_{q \in \mathcal{Q}} \lambda_q(\mathbf{a}_q)$, it is reinforced on all the edges of the best path $\mathcal{T}_{\text{best}}^{(i)}$ as $\varphi_{q,n}^{(i)} \leftarrow [\varphi_{q,n}^{(i)} + \Delta\varphi^{(i)}]_{\varphi_{\min}}^{\varphi_{\max}}$ $\forall e_{q,n} \in \mathcal{T}_{\text{best}}^{(i)}$, where $\Delta\varphi^{(i)} \triangleq \delta_{\varphi}\chi_{\text{best}}^{(i)}/\lambda_{\text{ELB}}^{\star}$, while $\varphi_{\min}$, $\varphi_{\max}$ and δ_{φ} are proper constants.

A few comments about the novel ACO-based solution to the SA-OP have to be emphasized: *i*) the rationale is first to "wisely" guarantee the maximization of the minimum ELB via a deterministic algorithm, and then, to iteratively improve this solution exploiting an intrinsically heuristic algorithm based on the ACO framework; *ii*) the thresholds $\varphi_{\min}$ and $\varphi_{\max}$, i.e., the minimum and maximum amount of pheromone allowed over each edge, respectively, allow the algorithm a minimum level of exploration over the graph edges in order to avoid premature ending of the search [28]; *iii*) the higher the ratio $\chi_{\text{best}}^{(i)}/\lambda_{\text{ELB}}^{\star}$, or equivalently, the better the current overall solution is when compared with that offered by the deterministic algorithm, the greater the amount of pheromone released on the edges of the best path; *iv*) the action of *reinforcement learning* made on the path $\mathcal{T}_{\text{best}}^{(i)}$ contributes to make it a bit more "privileged" (i.e., with temporary higher level of pheromone) among the others, so that at the subsequent iterations the corresponding edges will be selected with a slightly higher probability according to (19); *v*) at the end of the N_{it}th iteration, the path $\mathcal{T}_{\text{best}}^{(N_{\text{it}})}$ with the best EGP value $\chi_{\text{best}}^{(N_{\text{it}})}$ will give the solution $\mathbf{a}^{\star} = \mathbf{a}_{\text{best}}^{(N_{\text{it}})}$ to the SA-OP (12); *vi*) the required computational effort is linear in the number of vertices N, with order $\mathcal{O}(N+C)$ [34], with C depending on both the number of agents N_{a} and the edges per vertex $Q+1$.

VI. Simulation Results

In this section, after comparing the optimal B&B and the heuristic ACO-based algorithms for the solution to the SA-OP, we discuss the issues concerning the initialization and parameter setting of the MMG algorithm, and then, we focus on the overall performance of the proposed MMG-based RA (MMG-RA) strategy. To the best of authors' knowledge, due to the lack of similar algorithms in the literature addressing the topic of interest, we will take as performance benchmark a RA algorithm which is employed to initialize the MMG algorithm itself, referred to in the sequel as heuristic RA (H-RA) (see Sect. VI-D).

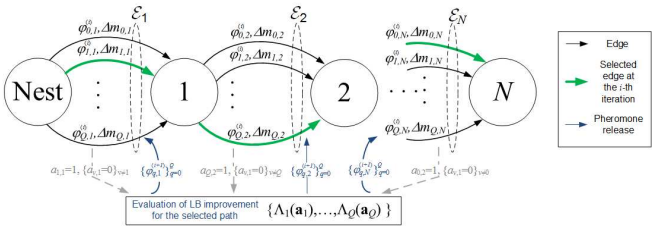

Fig. 2. ACO graph.

A. System Setup. The BIC-OFDMA system adopts $N = 64$ subcarriers spanning a bandwidth $B = 20\,\text{MHz}$. For each user with index $q \in \mathcal{Q}$, the transmitted packet[9] is made up of $N_q^{(\text{p})} = 1024$ and $N_q^{(\text{CRC})} = 32$ payload and CRC bits, respectively. The signaling format is based on a 64-state convolutional code, punctured according to the coding rate selected from the set $\mathcal{D}_{\text{r}} = \{1/2, 2/3, 3/4, 5/6\}$, and the modulation order can be 4-, 16- or 64-QAM, corresponding to $\mathcal{D}_{\text{m}} \triangleq \{2, 4, 6\}$, while a multiple-channel stop-and-wait ARQ scheme is employed with 8 logical channels. The transmit power available at the BS is $P = 34\,\text{dBm}$ and the noise power at the users' receiver over the bandwidth B is $P_N = -100$ dBm. Concerning the propagation channel, we assume the path-loss model compliant with the IEEE 802.16 non-line-of-sight urban scenario model and a short-term fading model with ITU pedestrian B power profile. The best fitting values of the pair $(\sigma_r; \gamma_{0,r})$ about the PER model of Sect. V-C are given in Tab. V. Additionally, the GP metrics, each obtained averaging over 10^3 independent channel realizations, are normalized by the ratio B/Q, having thus the meaning of spectral efficiencies (bit/s/Hz), and are plotted as a function of the average-symbol-energy-to-noise-spectral-density ratio E_s/N_0 of the user specified in the figure. Note that In all the numerical simulations, the AGP is estimated according its definition when the users' packets are transmitted over a realistic time-variant channel model, while the EGP is only used (as objective function) at the BS to analytically drive the selection of the best TM

B. B&B and ACO Algorithms for the SA-OP[10]. Figure 3 shows

[9] W.l.g., the header section of the packet has been skipped.

SA-OP-ACO algorithm

Input: N_{it}, N_{a}, $\varphi_{\min}$, $\varphi_{\max}$, δ_{φ}, ρ, λ_{ELB}^{*}
Initialize: $\varphi_{q,n}^{(0)}$, $\forall q \in \mathcal{Q}$, $\forall n \in \mathcal{N}$
For $i = 1 : N_{\text{it}}$
  For $j = 1 : N_{\text{a}}$
    Construct paths $\mathcal{T}_j^{(i)}$
  End For
  Evaluate $\chi_{\text{best}}^{(i)}$, $\mathcal{T}_{\text{best}}^{(i)}$, $\mathbf{a}_{\text{best}}^{(i)}$
  Pheromone evaporation $\varphi_{q,n}^{(i)} \leftarrow [(1-\rho)\varphi_{q,n}^{(i-1)}]_{\varphi_{\min}}^{\varphi_{\max}}$, $\forall q \in \mathcal{Q}$, $\forall n \in \mathcal{N}$
  Update $\pi_{q,n}$, $\forall q \in \mathcal{Q}$, $\forall n \in \mathcal{N}$
  If $\chi_{\text{best}}^{(i)} > \lambda_{\text{ELB}}^{*}$
    Evaluate $\Delta\varphi^{(i)}$
    Pheromone reinforcement $\varphi_{q,n}^{(i)} \leftarrow [\varphi_{q,n}^{(i)} + \Delta\varphi^{(i)}]_{\varphi_{\min}}^{\varphi_{\max}}$, $\forall e_{q,n} \in \mathcal{T}_{\text{best}}^{(i)}$
  End If
End For
Output: $\mathbf{a}^{\star} = \mathbf{a}_{\text{best}}^{(N_{\text{it}})}$

TABLE IV

	$r = 1/2$	$r = 2/3$	$r = 3/4$	$r = 5/6$
σ_r	10	7	5	4
$\gamma_{0,r}$	0.7198	1.064	1.309	1.633

TABLE V

Best fitting values for the PER model in Sect. V-C.

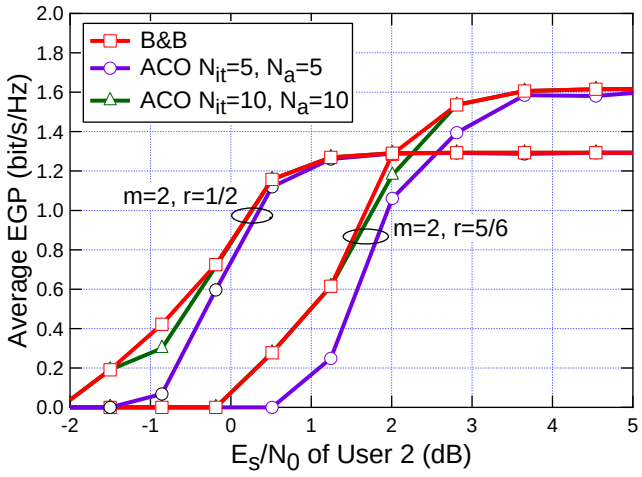

Fig. 3. Comparison of B&B and ACO algorithms when solving the SA-OP.

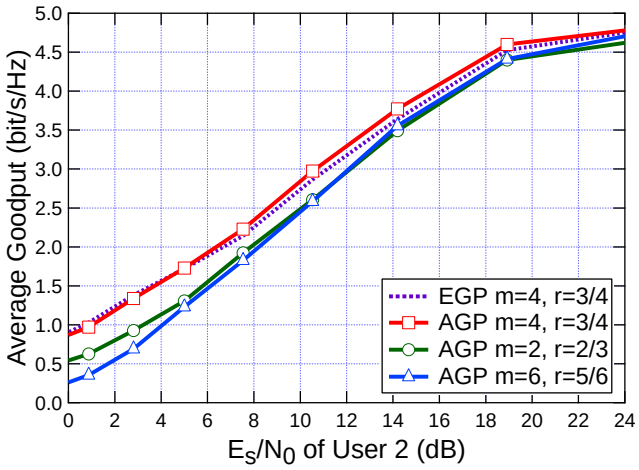

Fig. 4. AGP and EGP for different initialization pair of $\{m, r\}$.

the minimum average EGP obtained by solving the SA-OP when adopting either the optimal B&B or the ACO algorithm. We refer to the case of $Q = 2$ users, with the EGP being plotted versus the E_s/N_0 of user 2 with user 1 working at fixed $E_s/N_0 = 27$ dB. Two TPs configurations are chosen, i.e., $\{m_q, r_q\} = \{2, 1/2\}$ and $\{m_q, r_q\} = \{2, 5/6\}$, $q = 1, 2$, both of them with uniform PA. As for the ACO algorithm, two settings are employed, namely, $N_{\rm it} = 5$ with $N_{\rm a} = 5$, or $N_{\rm it} = 10$ with $N_{\rm a} = 10$. Interestingly, the performance of the ACO operating with $N_{\rm it} = 10$, $N_{\rm a} = 10$ is very close to that offered by the B&B, in spite of requiring a significant much lower computational complexity.

C. ACO Parameter Setup. Concerning the tuning of the parameters employed by the ACO algorithm, extensive simulations quantifying the overall performance of the MMG algorithm suggest that a suitable setting is given by $\rho = 0.1$, $\delta_\varphi = 0.1$, $\varphi_{\min} = 0.1/(N \cdot Q)$, $\varphi_{\max} = 5$, $N_{\rm it} = 50$ and $N_{\rm a} = 50$.

D. Initialization of the MMG Algorithm. The TP vector $\boldsymbol{\tau}_0$ required to initialize the MMG algorithm is found by applying the H-RA procedure, as outlined in the sequel.

1) As for the SA, each user picks up in a round-robin way the subcarrier with the best channel gain among the ones not yet allocated. This is in line with the result that the PER is dominated by the term corresponding to the worst channel gain [24].

2) The BS transmit power is uniformly distributed over all the subcarriers. The choice is made for simplicity, yet it reveals nearly optimal at high SNRs [12].

3) The three AGPs curves in Fig. 4 are obtained by the MMG algorithm initialized with the SA and PA described in 1) and 2), and $\{2, 2/3\}$, $\{4, 3/4\}$ and $\{6, 5/6\}$ as modulation and coding pair $\{m, r\}$; it is shown that the configuration $\{4, 3/4\}$ gives the best tradeoff between data rate and link reliability for the whole E_s/N_0 range on interest. Accordingly, the pair $\{4, 3/4\}$ will be chosen as the initial modulation and coding format each user employs on own subcarriers[11].

4) In order to find the best succession the CAM-based MMG algorithm has to follow to solve the SA-OP, PA-OP and AMC-OP subproblems, we have checked different options, as illustrated in Tab. VI. As apparent, the AMC-PA-SA sequence has to be preferred in that it gives the highest percentage of cases providing the best EGP performance. In conclusion, let us remark that simulation runs, carried out under various configurations, demonstrate that (the results are not reported due to limitation of space) 3-4 CAM iterations are enough to get the most significant improvement in the minimum EGP as well as AGP, thereby contributing to keep the overall complexity of the MMG-RA at affordable levels.

E. Performance of the MMG Algorithm. The average AGP metrics obtained for $Q = 3$ users either applying the proposed MMG-RA or the benchmark H-RA are quantified in Fig. 5 versus the E_s/N_0 of user 2, while users 1 and 3 are working at fixed $E_s/N_0 = 27$ dB and $E_s/N_0 = 7$ dB, respectively. The results demonstrate that the H-RA (solid marks) can favorably handle user 2 at high SNRs only, whereas the MMG-RA makes all the users to experience the same AGP, in line with the maximum fairness criterion adopted by the OP. Figure 6 addresses a scenario composed of a maximum of $Q = 6$ users randomly located within the BS coverage, each operating at a

[10]The aim of Sects. VI-B and VI-C is to test the effectiveness of the sub-optimal ACO algorithm against the optimal B&B one, and to tune the ACO parameter setup, respectively. In these sections, therefore, we focus on the solution of the SA-OP only, without caring about the AMC and PA subproblems.

[11]For simplicity, the EGP curves for the setups $\{2, 2/3\}$ and $\{6, 5/6\}$ have been not depicted. It is, however, interesting to emphasize that all the EGP curves of Fig. 4 turn out to be very close to the corresponding AGP ones obtained by simulations, thus proving the accuracy of the performance model developed in Sect. III-A.

AMC-PA-SA	AMC-SA-PA	PA-AMC-SA	PA-SA-AMC
45.65%	21.74%	17.39%	15.22%

TABLE VI

SEQUENCES OF ALGORITHMS TO BE SOLVED FOR THE MMG PROBLEM AND % OF CASES WHERE THEY ACHIEVE THE BEST MIN. EGP.

E_s/N_0 User 2 (dB)	2.8	5	7.5	10.5	14
QoS Constrained	0.0093	0.0093	0.0084	0.0031	0.001
No QoS Constrained	0.0759	0.0405	0.0205	0.0062	0.001

TABLE VII

PER VS. E_s/N_0 FOR USER 2 WITH ($\Upsilon_2 = 10^{-2}$) AND WITHOUT PER QOS CONSTRAINT.

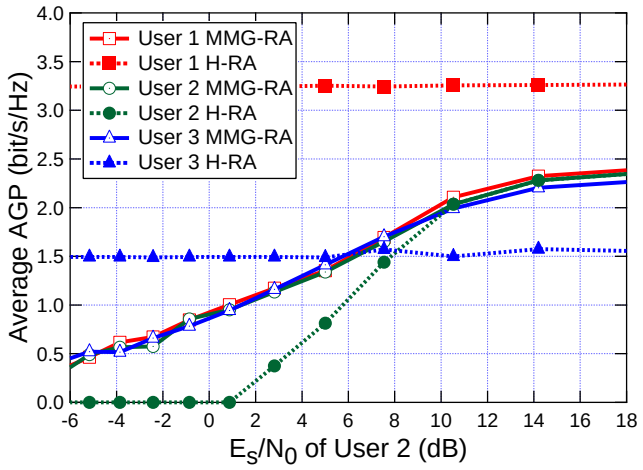

Fig. 5. AGP of $Q = 3$ users for the MMG-based and heuristic RAs.

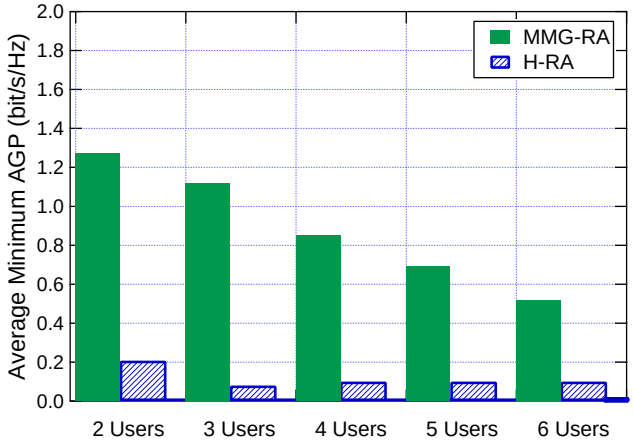

Fig. 6. Average minimum AGP for different number of users Q.

different E_s/N_0 (namely, 8.6, 7.5, 10.5, 6.4, 9.8 and 5.9 dB), evaluated according to the channel model and the path loss. As expected, the average minimum AGP offered by the MMG-RA decreases as Q increases, since the same resources have to be shared by more and more users. Nevertheless, the MMG-RA algorithm considerably outperforms the H-RA, thus exhibiting a considerable intrinsic robustness against the network load Q. Finally, the MMG-RA capability of satisfying the QoS constraint (4.c) has been corroborated through simulations performed in various scenarios. A typical result is quantified in Tab. VII, where the PER of user 2 (user 1 works at E_s/N_0 = 27 dB) evaluated under the QoS constraint stays all the time below the adopted threshold level $\Upsilon_2 = 10^{-2}$.

VII. Concluding Remarks

In this work, the cross-layer design of a novel RA strategy has been formulated as a nonlinear nonconvex mixed OP that maximizes the GP of the worst user in the downlink of an ARQ-based OFDMA system. The CAM method allows to avoid the prohibitive complexity of the original problem by decomposing it into the sequence of the AMC, PA and SA subproblems, each of which is iteratively and optimally solved. Specific effort has been put in the nonlinear integer combinatorial SA-OP, by first deriving an optimal yet computationally complex solution (and so, to be used as benchmark), and an alternative suboptimal yet efficient one based on the ACO framework. Numerical simulation results support and corroborate: *i*) the analytical findings; *ii*) the effectiveness of the ACO-based against the optimal method in solving the SA-OP; *iii*) the improved features of the proposed MMG-RA when compared to other works; *iv*) the capability of ensuring maximum fairness among users; *v*) the optimization of the BS resources when practical AMC schemes are adopted; *vi*) the improvement of the system GP efficiency compared to heuristic RA strategies.

Appendix

A. Evaluation of the Goodput Metric

Given the sequence of the channel coefficients $\mathbf{h}_{\ell+1,q}, \cdots, \mathbf{h}_{L,q}$, the average time required to receive an error-free packet of the qth user within the L available PRs results to be the sum of the interval $\Delta_{\ell-1,q}$ spent in the previous $\ell-1$, $1 \le \ell \le L$, failed transmissions (*failure time*) and the interval (*successful time*)

$$D_{\ell,q}(\boldsymbol{\sigma}_{\ell,q}, \cdots, \boldsymbol{\sigma}_{L,q}) \triangleq \sum_{i=0}^{L-\ell} \left\{ \left[\sum_{v=0}^{i} T_{\ell+v,q}^{(\mathrm{u})} \right] \cdot \left[1 - \Gamma_{r_{\ell+i,q}}(\boldsymbol{\sigma}_{\ell+i,q})\right] \prod_{j=-1}^{i-1} \Gamma_{r_{\ell+j,q}}(\boldsymbol{\sigma}_{\ell+j,q}) \right\} \quad (20)$$

where $\Gamma_{r_{k,q}}(\boldsymbol{\sigma}_{k,q})$ denotes the PER of user q at PR k when the TPs vector $\boldsymbol{\tau}_{k,q}$ is used, with $\Gamma_{r_{\ell-1,q}}(\boldsymbol{\sigma}_{\ell-1,q}) \triangleq 1$ and $\boldsymbol{\sigma}_{k,q} \triangleq \{\boldsymbol{\tau}_{k,q} \,|\, \mathbf{h}_{k,q}\}$, $\ell \le k \le L$, whereas $T_{\ell,q}^{(\mathrm{u})} \triangleq \frac{T_{\mathrm{B}} N_q^{(\mathrm{u})}}{r_{\ell,q} m_{\ell,q} \sum_{n \in \mathcal{N}} a_{\ell,q,n}}$ is the interval to transmit a packet of $N_q^{(\mathrm{u})}$ bits employing at PR ℓ the TPs $\boldsymbol{\tau}_{\ell,q}$, T_{B} being the OFDM symbol duration. The *average GP* (measured in bits per OFDM symbol) at PR ℓ for user q can thus be evaluated over M packet transmissions as

$$\overline{\Xi}_{\ell,q}^{(M)} = \frac{T_{\mathrm{B}} N_q^{(\mathrm{p})}}{\frac{1}{M} \sum_{m=1}^{M} \left[\Delta_{\ell-1,q}^{(m)} + D_{\ell,q}(\boldsymbol{\sigma}_{\ell,q}^{(m)}, \cdots, \boldsymbol{\sigma}_{L,q}^{(m)}) \right]}, \quad (21)$$

where $\Delta_{\ell-1,q}^{(m)}$ and the RV $D_{\ell,q}(\boldsymbol{\sigma}_{\ell,q}^{(m)}, \cdots, \boldsymbol{\sigma}_{L,q}^{(m)})$ denote the failure time and the average successful time corresponding to the mth packet, respectively. Hence, the *long-term average GP* can be obtained as $\lim_{M\to\infty} \overline{\Xi}_{\ell,q}^{(M)}$. Thus, exploiting the law of large numbers, the denominator of (21) turns into $\overline{\Delta}_{\ell-1,q} + \mathrm{E}\{D_{\ell,q}(\boldsymbol{\sigma}_{\ell,q}, \cdots, \boldsymbol{\sigma}_{L,q})\}$, where $\overline{\Delta}_{\ell-1,q}$ is the average failure time and $\mathrm{E}\{D_{\ell,q}(\boldsymbol{\sigma}_{\ell,q}, \cdots, \boldsymbol{\sigma}_{L,q})\}$ is the expected value, taken over the *future* channel coefficients $\mathbf{h}_{\ell+1,q}, \cdots, \mathbf{h}_{L,q}$, of the successful time for delivering a given error-free packet, provided that $L-\ell+1$ PRs are still available. However, since the expectation $\mathrm{E}\{D_{\ell,q}\}$ is computationally impractical to evaluate in closed-form, we resort to the long-term static channel assumption [15], [24], meaning that the packet is assumed to experience current channel conditions $\mathbf{h}_{\ell,q}$ also during its possible future retransmissions, i.e., $\mathbf{h}_{\ell,q} = \mathbf{h}_{\ell+1,q} = \cdots = \mathbf{h}_{L,q}$.

Now, let us introduce the following definition followed by an useful proposition.

Definition 7: The sequence x_ℓ is a *Martingale* relative to the class $\mathcal{F}_\ell$ of all the relevant past events up to and including time ℓ, with $\ell \geq 1$, if each x_ℓ has an expectation and if for $n > \ell$ [35]

$$\mathrm{E}\left\{x_n \,|\mathcal{F}_\ell\right\} = x_\ell. \tag{22}$$

Proposition 4: The sequence $x_\ell \triangleq \Gamma_{r_{\ell,q}}(\boldsymbol{\sigma}_{\ell,q})$ turns out a Martingale relative to the class $\mathcal{F}_\ell \triangleq \boldsymbol{\sigma}_{\ell,q}$.

As a consequence, since $\mathbf{h}_{\ell,q}$ is currently known and in view of the above proposition, we can let

$$\mathrm{E}\left\{\Gamma_{r_{\ell+i,q}}(\boldsymbol{\sigma}_{\ell+i,q})\right\} = \Gamma_{r_{\ell,q}}(\boldsymbol{\sigma}_{\ell,q}), \;\; 1 \leq i \leq L-\ell. \tag{23}$$

The following remarks motivate and substantiate this result.

1) The resulting EGP objective function is analytically simple and does not require side information, e.g., the estimate of delay spread, Doppler bandwidth and so on, required for complex channel prediction techniques.
2) This is a well-known assumption, commonly adopted in the literature; see [36] and [37].
3) As apparent from the numerical results (see for instance Fig. 4), despite its simplicity, the EGP, provides an accurate estimate of the AGP over realistic wireless environments.

By applying the martingale-ness property (23) of $\Gamma_{r_{\ell,q}}(\boldsymbol{\sigma}_{\ell,q})$ to (21), we get

$$\begin{aligned}&\mathrm{E}\{D_{\ell,q}(\boldsymbol{\sigma}_{\ell,q},\cdots,\boldsymbol{\sigma}_{L,q})\} = \mathrm{E}\{D_{\ell,q}(\boldsymbol{\sigma}_{\ell,q})\}\\ &= T^{(\mathrm{u})}_{\ell,q}\cdot\frac{1-\Gamma_{r_{\ell,q}}(\boldsymbol{\sigma}_{\ell,q})}{\Gamma_{r_{\ell,q}}(\boldsymbol{\sigma}_{\ell,q})}\sum_{i=0}^{L-\ell}(i+1)\left[\Gamma_{r_{\ell,q}}(\boldsymbol{\sigma}_{\ell,q})\right]^{i+1}.\end{aligned} \tag{24}$$

After some algebra, (24) can be upper bounded as $\mathrm{E}\{D_{\ell,q}(\boldsymbol{\sigma}_{\ell,q})\} \leq \dfrac{T^{(\mathrm{u})}_{\ell,q}}{1-\Gamma_{r_{\ell,q}}(\boldsymbol{\sigma}_{\ell,q})}$, and accordingly, the LB of the long-term average GP results as

$$\Xi_{\ell,q}(\boldsymbol{\sigma}_{\ell,q}) \geq \left[\frac{\overline{\Delta}_{\ell-1,q}}{T_{\mathrm{B}}N^{(\mathrm{p})}_q}+\frac{T^{(\mathrm{u})}_{\ell,q}}{T_{\mathrm{B}}N^{(\mathrm{p})}_q(1-\Gamma_{r_{\ell,q}}(\boldsymbol{\sigma}_{\ell,q}))}\right]^{-1}. \tag{25}$$

Summing up, since we are interested to solve the MMG-OP, the minimum of $\Xi_{\ell,q}(\boldsymbol{\sigma}_{\ell,q})$ in (25) over $q \in \mathcal{Q}$ coincides with that of the metric defined in (2) after recalling the definition of $\boldsymbol{\sigma}_{\ell,q}$ and $T^{(\mathrm{u})}_{\ell,q}$ given above.

B. Subgradient Method for the Dual OP (10)

To maximize $g(\boldsymbol{\Theta})$ in (10), the subgradient method updates at the step $i+1$ the components of the dual variable $\boldsymbol{\Theta}^{(i)}$ produced at the previous step i along the search direction defined by the gradient $\nabla_{\boldsymbol{\Theta}} g(\boldsymbol{\Theta}^{(i)}) = \mathbf{d}(\mathbf{p})|_{\mathbf{p}=\mathbf{p}(\boldsymbol{\Theta}^{(i)})}$, according toTab. III. The step size δ is chosen sufficiently small to allow the algorithm to converge. Denoting with X_k, $1 \leq k \leq |\boldsymbol{\Theta}|$, then the component of the update of $\boldsymbol{\Theta}^{(i)}$ at the step $i+1$, the component-wise projection results as $[X_k]_{\mathcal{D}_{\boldsymbol{\Theta}}} = \max\{0, X_k\}$, $\forall X_k$ projected over $\mathcal{D}_\theta$ or $\mathcal{D}_\phi$, whereas $[X_k]_{\mathcal{D}_{\boldsymbol{\Theta}}} = \max\{0, X_k+\varepsilon_\omega\}$, $\forall X_k$ projected over $\mathcal{D}_\omega \cap \mathcal{D}_{\bar{\omega}}$, being the scalar ε_ω found by solving $\sum_{k|X_k\in\mathcal{D}_\omega\cap\mathcal{D}_{\bar{\omega}}} \max\{0, X_k+\varepsilon_\omega\} = 1$ via the bisection method.

C. Ant Colony Optimization Primer

The ACO framework is an efficient tool for solving combinatorial OPs (COPs) modeled as $\mathcal{P} = \{\mathcal{S}, \Omega, f\}$, where $\mathcal{S}$ is the discrete search space over D decision variables $x_i \in \mathcal{X}_i \triangleq \{d_i^{(1)}, \cdots, d_i^{(|\mathcal{X}_i|)}\}$, $1 \leq i \leq D$, Ω is the set of constraints among the D decision variables, and $f : \mathcal{S} \to \mathbb{R}^+$ is the objective function [28]. The ACO algorithm is applied by mapping the COP of interest onto the graph $\mathsf{G}(\mathcal{V}, \mathcal{E})$, where $\mathcal{V}$ and $\mathcal{E}$ are the set of vertices and edges, respectively. A feasible solution, i.e., one consisting of a complete assignment of the variables $x_i \in \mathcal{X}_i$ while satisfying the set of constraints Ω, is associated to a path $\mathcal{T}$ on the graph, where all the vertices are connected and each vertex is visited only once. Assuming that the decision variables correspond to the graph edges, the ACO solution is found by making N_{a} independent agents explore the graph for a number N_{it} of times. At each exploration, the agent of index a, $1 \leq a \leq N_a$: *i*) builds a feasible solution starting from $\mathcal{T}^{(a)} = \emptyset$ and randomly selecting the initial vertex; *ii*) selects with probability $\pi_{i,j}$ the edge $e_{i,j} \in \mathcal{N}_e$, where $\mathcal{N}_e$ is the set of edges connecting the vertices not visited yet, and then moves from vertex i to vertex j; *iii*) updates the path set $\mathcal{T}^{(a)} \leftarrow \mathcal{T}^{(a)} \cup \{e_{i,j}\}$ and the edge set $\mathcal{N}_e \leftarrow \mathcal{N}_e \backslash \{e_{i,j}\}$; *iv*) continues until a complete path, i.e., a feasible solution, is obtained. Upon defining the *local desirability* $\eta_{i,j}$ as a quantity locally associated to the relevant edge and the *pheromone* $\varphi_{i,j}$ as depending on the quality of the global solution that specific edge contributes to, we recall: *i*) $\pi_{i,j}$ depends on both $\eta_{i,j}$ and $\varphi_{i,j}$; *ii*) at the end of each iteration, the pheromone evaporates over all the edges at rate ρ, i.e., $\varphi_{i,j} \leftarrow (1-\rho)\varphi_{i,j}$; *iii*) the agent that has found the best solution $\mathcal{T}_{\mathrm{best}}$, i.e., the one returning the best value of the objective function f while satisfying the constraints, increases the pheromone by $\Delta\varphi$ over the edges $e_{i,j} \in \mathcal{T}_{\mathrm{best}}$; *iv*) at the end of N_{it} iterations, a stable path emerges on the graph, which gives the best solution to the COP found so far.

REFERENCES

[1] M. Sternad, T. Svensson, T. Ottosson, A. Ahlen, A. Svensson, and A. Brunstrom, "Towards systems beyond 3G based on adaptive OFDMA transmission," *Proc. IEEE*, vol. 95, no. 12, pp. 2432–2455, Dec 2007.

[2] A. Ghosh, N. Mangalvedhe, R. Ratasuk, B. Mondal, M. Cudak, E. Visotsky, T. Thomas, J. Andrews, P. Xia, H. Jo, H. Dhillon, and T. Novlan, "Heterogeneous cellular networks: From theory to practice," *IEEE Commun. Mag.*, vol. 50, no. 6, pp. 54–64, June 2012.

[3] J. Andrews, S. Buzzi, W. Choi, S. Hanly, A. Lozano, A. Soong, and J. Zhang, "What will 5G be?" *IEEE J. Select. Areas Commun.*, vol. 32, no. 6, pp. 1065–1082, June 2014.

[4] G. Song and Y. Li, "Utility-based resource allocation and scheduling in OFDM-based wireless broadband networks," *IEEE Commun. Mag.*, vol. 43, no. 12, pp. 127–134, Dec 2005.

[5] K. Letaief and Y. J. Zhang, "Dynamic multiuser resource allocation and adaptation for wireless systems," *IEEE Wireless Commun.*, vol. 13, no. 4, pp. 38–47, Aug 2006.

[6] C. Y. Wong, R. Cheng, K. Lataief, and R. Murch, "Multiuser OFDM with adaptive subcarrier, bit, and power allocation," *IEEE J. Select. Areas Commun.*, vol. 17, no. 10, pp. 1747–1758, Oct 1999.

[7] J. Jang and K. B. Lee, "Transmit power adaptation for multiuser OFDM systems," *IEEE J. Select. Areas Commun.*, vol. 21, no. 2, pp. 171–178, Feb 2003.

[8] Z. Shen, J. Andrews, and B. Evans, "Adaptive resource allocation in multiuser OFDM systems with proportional rate constraints," *IEEE Trans. Wireless Commun.*, vol. 4, no. 6, pp. 2726–2737, Nov 2005.

[9] W. Rhee and J. Cioffi, "Increase in capacity of multiuser OFDM system using dynamic subchannel allocation," in *IEEE Veh. Technol. Conf. (VTC 2000)*, vol. 2, May 2000, pp. 1085–1089.

[10] I. Kim, I.-S. Park, and Y. H. Lee, "Use of linear programming for dynamic subcarrier and bit allocation in multiuser OFDM," *IEEE Trans. Veh. Technol.*, vol. 55, no. 4, pp. 1195–1207, July 2006.

[11] C. Bae and D.-H. Cho, "Fairness-aware adaptive resource allocation scheme in multihop OFDMA systems," *IEEE Commun. Lett.*, vol. 11, no. 2, pp. 134–136, Feb 2007.

[12] T. Wang and L. Vandendorpe, "Iterative resource allocation for maximizing weighted sum min-rate in downlink cellular OFDMA systems," *IEEE Trans. Signal Processing*, vol. 59, no. 1, pp. 223–234, Jan 2011.

[13] G. Caire, G. Taricco, and E. Biglieri, "Bit-interleaved coded modulation," *IEEE Trans. Inform. Theory*, vol. 44, no. 3, pp. 927–946, May 1998.

[14] D. P. Bertsekas and R. Gallager, *Data Networks.* 2nd edition. Prentice Hall, 2002.

[15] D. Qiao, S. Choi, and K. Shin, "Goodput analysis and link adaptation for IEEE 802.11a wireless LANs," *IEEE Trans. Mobile Comput.*, vol. 1, no. 4, pp. 278–292, Oct 2002.

[16] R. Aggarwal, M. Assaad, C. Koksal, and P. Schniter, "Joint scheduling and resource allocation in the OFDMA downlink: Utility maximization under imperfect channel-state information," *IEEE Trans. Signal Processing*, vol. 59, no. 11, pp. 5589–5604, Nov 2011.

[17] D. Ng and R. Schober, "Cross-layer scheduling for OFDMA amplify-and-forward relay networks," *IEEE Trans. Veh. Technol.*, vol. 59, no. 3, pp. 1443–1458, March 2010.

[18] R. Aggarwal, C. Koksal, and P. Schniter, "Joint scheduling and resource allocation in OFDMA downlink systems via ACK/NAK feedback," *IEEE Trans. Signal Processing*, vol. 60, no. 6, pp. 3217–3227, June 2012.

[19] Z. Ho, V. Lau, and R. Cheng, "Cross-layer design of FDD-OFDM systems based on ACK/NAK feedbacks," *IEEE Trans. Inform. Theory*, vol. 55, no. 10, pp. 4568–4584, Oct 2009.

[20] D. Hui and V. Lau, "Design and analysis of delay-sensitive cross-layer OFDMA systems with outdated CSIT," *IEEE Trans. Wireless Commun.*, vol. 8, no. 7, pp. 3484–3491, July 2009.

[21] ——, "Design and analysis of delay-sensitive decentralized cross-layer OFDMA systems with efficient feedback algorithm," *IEEE Trans. Wireless Commun.*, vol. 8, no. 12, pp. 5844–5851, Dec 2009.

[22] J. Escudero-Garzas, B. Devillers, and A. Garcia-Armada, "Fairness-adaptive goodput-based resource allocation in OFDMA downlink with ARQ," *IEEE Trans. Veh. Technol.*, vol. 63, no. 3, pp. 1178–1192, March 2014.

[23] I. Stupia, V. Lottici, F. Giannetti, and L. Vandendorpe, "Link resource adaptation for multiantenna bit-interleaved coded multicarrier systems," *IEEE Trans. Signal Processing*, vol. 60, no. 7, pp. 3644–3656, July 2012.

[24] R. Andreotti, I. Stupia, V. Lottici, F. Giannetti, and L. Vandendorpe, "Goodput-based link resource adaptation for reliable packet transmissions in BIC-OFDM cognitive radio networks," *IEEE Trans. Signal Processing*, vol. 61, no. 9, pp. 2267–2281, May 2013.

[25] D. P. Bertsekas, *Nonlinear Programming*. 2nd edition. Athena Scientific, 2003.

[26] S. Boyd and L. Vandenberghe, *Convex Optimization*. Cambridge Univ. Press, 2004.

[27] M. Brusco and S. Stahl, *Branch-and-Bound. Applications in Combinatorial Data Analysis*, ser. Statistics & Computing. Springer Verlag, 2005.

[28] M. Dorigo, M. Birattari, and T. Stützle, "Ant colony optimization," *IEEE Comput. Intell. Mag.*, vol. 1, no. 4, pp. 28–39, Nov 2006.

[29] R. Andreotti, I. Stupia, F. Giannetti, V. Lottici, and L. Vandendorpe, "Resource allocation in OFDMA underlay cognitive radio systems based on Ant Colony Optimization," in *2010 IEEE Eleventh Intern. Workshop on Signal Processing Advances in Wireless Commun. (SPAWC)*, June 2010, pp. 1–5.

[30] Y. Blankenship, P. Sartori, B. Classon, V. Desai, and K. Baum, "Link error prediction methods for multicarrier systems," in *IEEE 60th Veh. Technol. Conf. (VTC2004-Fall)*, vol. 6, Sept 2004, pp. 4175–4179.

[31] C. Flouda, *Nonlinear and Mixed-Integer Optimization: Fundamentals and Applications*. Oxford University Press, 1995.

[32] I. Stupia, F. Giannetti, V. Lottici, and L. Vandendorpe, "A greedy algorithm for goodput-based adaptive modulation and coding in BIC-OFDM systems," in *2010 European Wireless Conf. (EW)*, April 2010, pp. 608–615.

[33] P. Tsiaflakis, I. Necoara, J. Suykens, and M. Moonen, "Improved dual decomposition based optimization for DSL dynamic spectrum management," *IEEE Trans. Signal Processing*, vol. 58, no. 4, pp. 2230–2245, April 2010.

[34] Y. Liu, M. Tao, B. Li, and H. Shen, "Optimization framework and graph-based approach for relay-assisted bidirectional OFDMA cellular networks," *IEEE Trans. Wireless Commun.*, vol. 9, no. 11, pp. 3490–3500, Nov 2010.

[35] R. Heim, "On the algorithmic foundation of information theory," *IEEE Trans. Inform. Theory*, vol. 25, no. 5, pp. 557–566, Sep 1979.

[36] A. Goldsmith and S.-G. Chua, "Variable-rate variable-power MQAM for fading channels," *IEEE Trans. Commun.*, vol. 45, no. 10, pp. 1218–1230, Oct 1997.

[37] M.-S. Alouini and A. Goldsmith, "Capacity of Rayleigh fading channels under different adaptive transmission and diversity-combining techniques," *IEEE Trans. Veh. Technol.*, vol. 48, no. 4, pp. 1165–1181, Jul 1999.

Riccardo Andreotti received the BS and MS (summa cum laude) degree in Telecommunications Engineering from the University of Pisa, Italy, in 2007 and 2009, respectively, and the Ph.D. degree in Information Engineering from both the University of Pisa, Italy, and Universit catolique de Louvain, Louvain-la-Neuve, Belgium, in 2013. From 2013 to 2014 he held a postdoctoral position at the Department of Information Engineering of the University of Pisa. Since 2014 he has been with Wireless System Engineering and Research (WISER) S.r.l., Livorno, Italy. His research interests concern the areas of wireless communication and navigation systems and signal processing, including link performance prediction and resource allocation techniques for multicarrier systems, game theory application to distributed resource allocation problems in wireless communication systems, and design of innovative signal formats for future GNSS.

Tao Wang (M′10–SM′12) received Ph.D from Université Catholique de Louvain (UCL), Belgium in 2012, Doctor of Engineering and Bachelor degreesfrom Zhejiang University,China, in 2006 and 2001, respectively. He has been with Key Laboratory of SpecialtyFiber Opticsand Optical Access Networks, Shanghai University, China as a Professor since Feb. 2013. His current interest is in energy-efficient wireless communicationand signal processing systems. He received Professorof Special Appointment (Eastern Scholar) Awardfrom Shanghai MunicipalEducation Commission,as well as Best Paper Award in2013 InternationalConference onWireless Communications and Signal Processing.He is an associate editor for EURASIP Journalon Wireless Communicationsand Networking.He is an IEEE Senior Member

Vincenzo Lottici received the Dr. Ing. degree (summa cum laude) and the BTA in electrical engineering both from the University of Pisa in 1985 and 1986, respectively. From 1987 to 1993 he was engaged in the research of sonar digital signal processing algorithms. Since 1993 he has been with the Department of Information Engineering of the University of Pisa, where he is currently an Assistant Professor in Communication Systems. He participated in several international and national research projects, and as TPC member, in numerous IEEE conferences in wireless communications and signal processing, such as Globecom2016, ICC2016 Globecom2015, ICC2015, WCNC2015, ICUWB2015, Globecom2014, ICC2014, ICUWB2014, WCNC2014, APWiMob2014, ICC2013, Globecom2013, WCNC2013, ICUWB2013, WCNC2012, SPAWC2012, PIMRC2012, ICUWB2011, ICC2011, WCNC2011, ICASSP2010, PIMRC2010, WCNC2010, CIP2010, Globecom2009, SPAWC2009, EUSIPCO2006, Globecom2006. In 2013, he joined the Editorial Board of EURASIP Advances on Signal Processing. He received the Best Paper Award in 2006 for the work “A Theoretical Framework for Soft Information Based Synchronization in Iterative (Turbo) Receivers”, EURASIP Journal on Wireless Communications and Networking, April 2005, by the EU-funded project Network of Excellence in Wireless Communications (NEWCOM). He has authored more than 120 research papers on international journals and conferences in the broad area of signal processing for communications, with emphasis on synchronization, dynamic resource allocation, cognitive radio and compressive sensing

Filippo Giannetti received the Doctor Engineer (summa cum laude) and the Research Doctor degrees in electronic engineering from the University of Pisa, Italy, in 1989 and in 1993, respectively. In 1992 , he spent a research period with the European Space Agency Research and Technology Centre (ESA/ESTEC), Noordwijk, The Netherlands, where he was engaged in several activities in the field of digital satellite communications. From 1993 to 1998, he was a Research Scientist at the Department of Information Engineering , University of Pisa, where he is currently an Associate Professor of Telecommunications. His main research interests are in the field of wireless communications, with special emphasis on digital modem design, digital signal processing algorithms, wideband transmission techniques, and resource allocation in cognitive and cooperative networks.

Luc Vandendorpe (M′93–SM′99–F′06) was born in Mouscron, Belgium, in 1962. He received thedegree (summa cum laude) in electrical engineering and the Ph.D. degree from the Universit Catholiquede Louvain (UCL), Louvain La Neuve, Belgium, in 1985 and 1991, respectively. Since 1985, hehas been with the Communications and Remote Sensing Laboratory, UCL, where he rst worked inthe eld of bit rate reduction techniques for video coding. In 1992, he was a Visiting Scientist anda Research Fellow at the Telecommunications and Trafc Control Systems Group, Delft Technical University, the Netherlands, where he worked on spread spectrum techniques for personal communications systems. From October 1992 to August 1997, he was a Senior Research Associate of the Belgian NSF, UCL, and an invited Assistant Professor. He is now a Full Professor with the Institute for Information and Communication Technologies, Electronics, and Applied Mathematics, UCL. His research interests include digital communication systems and more precisely resource allocation for OFDM(A)-based multicell systems, MIMO and distributed MIMO, sensor networks, turbo-based communications systems, physical layer security, and UWB-based positioning. He is a TPC Member for numerous IEEE conferences (VTC, Globecom, SPAWC, ICC, PIMRC, and WCNC) and for the Turbo Symposium. He was a Co-Technical Chair for the IEEE ICASSP 2006. He served as an Editor for Synchronization and Equalization of the IEEE TRANSACTIONS ON COMMUNICATIONS between 2000 and 2002, and as an Associate Editor of the IEEE TRANSACTIONS ON WIRELESS COMMUNICATIONS between 2003 and 2005, and the IEEE TRANSACTIONS ON SIGNAL PROCESSING between 2004 and 2006. He was the Chair of the IEEE Benelux joint chapter on communications and vehicular technology between 1999 and 2003. He was an elected member of the Signal Processing for Communications Committee between 2000 and 2005, and an elected member of the Sensor Array and Multichannel Signal Processing Committee of the Signal Processing Society between 2006 and 2008, and between 2009 and 2011. He is the Editor-in-Chief for the EURASIP Journal on Wireless Communications and Networking. He was a corecipient of the 1990 Biennal Alcatel-Bell Award from the Belgian NSF for a contribution in the eld of image coding. In 2000, he was corecipient (with J. Louveaux and F. Deryck) of the Biennal Siemens Award from the Belgian NSF for a contribution about lter-bank-based multicarrier transmission.